

Analysis of Visual Field Reports for Diagnosis of Glaucoma



By

Fareena Fatima

NUST201464504MCEME35214F

Supervisor

Dr. Muhammad Usman Akram

Department of Computer Engineering
College of Electrical and Mechanical Engineering (CEME)
National University of Sciences and Technology (NUST)
Islamabad, Pakistan

July 2018

Analysis of Visual Field Reports for Diagnosis of Glaucoma

Author

Fareena Fatima

NUST201464504MCEME35214F

A thesis submitted in partial fulfillment of the requirements for the
degree of

MS Computer Engineering

Thesis Supervisor

Dr. Muhammad Usman Akram

Thesis Supervisor Signature: _____

Department of Computer Engineering
College of Electrical and Mechanical Engineering (CEME)
National University of Sciences and Technology (NUST)
Islamabad, Pakistan

July 2018

Declaration

I, *Fareena Fatima* declare that this thesis titled “Analysis of Visual Field Reports for Diagnosis of Glaucoma” and the work presented in it are my own and has been generated by me as a result of my own original research.

I confirm that:

1. This work was done wholly or mainly while in candidature for a Master of Science degree at NUST
2. Where any part of this thesis has previously been submitted for a degree or any other qualification at NUST or any other institution, this has been clearly stated
3. Where I have consulted the published work of others, this is always clearly attributed
4. Where I have quoted from the work of others, the source is always given. With the exception of such quotations, this thesis is entirely my own work
5. I have acknowledged all main sources of help
6. Where the thesis is based on work done by myself jointly with others, I have made clear exactly what was done by others and what I have contributed myself

Fareena Fatima

NUST201464504MCEME35214F

Language Correctness Certificate

This thesis has been read by an English expert and is free of typing, syntax, semantic, grammatical and spelling mistakes. Thesis is also according to the format given by the university.

Signature of Student

Fareena Fatima

NUST201464504MCEME35214F

Signature of Supervisor

Dr. Muhammad Usman Akram

Copyright Notice

- Copyright in text of this thesis rests with the student author. Copies (by any process) either in full, or of extracts, may be made only in accordance with instructions given by the author and lodged in the Library of CEME, NUST. Details may be obtained by the Librarian. This page must form part of any such copies made. Further copies (by any process) may not be made without the permission (in writing) of the author.
- The ownership of any intellectual property rights which may be described in this thesis is vested in CEME, NUST, subject to any prior agreement to the contrary, and may not be made available for use by third parties without the written permission of CEME, which will prescribe the terms and conditions of any such agreement.
- Further information on the conditions under which disclosures and exploitation may take place is available from the Library of CEME, NUST, Rawalpindi.

Dedicated to *my beloved husband , adorable kids and supportive
Mother in Law*

Abstract

Glaucoma is the second leading cause of blindness in the world, according to the World Health Organization, the first being cataracts. Everyone is at risk for glaucoma from babies to senior citizens. Glaucoma is an eye disease that is characterized by a particular pattern of progressive damage to the optic nerve that generally begins with a subtle loss of side vision (peripheral vision). Elevated pressure in the eye is the main factor leading to glaucomatous damage to the eye (optic) nerve. If not diagnosed and treated, it can progress to loss of central vision and blindness causing an irreversible damage. Glaucoma usually causes no symptoms early in its course, at which time it can only be diagnosed by regular eye examinations. Visual fields are used to diagnose the presence of glaucoma and monitor its progression. The blind spots created in the patient's eye by glaucoma can be seen on the visual field map. This type of test is known as Standard Automated Perimetry (SAP). There are various types of SAP, but the most commonly used is Humphrey. In this thesis we use image processing and decision support techniques to automate the analysis of visual field reports in order to aid ophthalmologists. The main focus is extract, locate and score quantitatively the glaucomatous damage in each hemisphere so that the extent of damage may be known. The pattern deviation (PD) plot printed in the visual field test report contains the significantly depressed points referred to as probability key symbols (PKS); whose shape, location in ISNT regions and count give us information about the damage caused by glaucoma to the optic nerve. Our thesis focuses on the extraction, location region, count and score of these PKSs in the upper and lower hemispheres of the PD plot hence automating the scoring of the analysis of visual field tests.

Keywords: *Humphrey Visual Field, Glaucoma, Standard Automated Perimetry*

Acknowledgments

All praise to be Allah, who gives courage to a weak man to fulfill things that are utterly in HIS MIGHTY control.

I would like to express sincere gratitude to my supervisor Dr. Usman Akram, whose professionalism guided me in the right direction and whose upright character made me learn priceless morals. Also, I am thankful to my co-supervisor Dr. Shoab Akram, who is a living legend of our academic era and I am blessed to be his student along with special acknowledgment to my entire thesis committee: Dr. Arslan Shoukat and Dr. Farhan Hussain.

Special thanks to Dr. Wajiha Rasool of BBH Hospital for giving me time from her very busy schedule and explaining me the medical concepts related to the visual field test reports and for also authenticating my results.

My thesis could not have been completed without the following people: Sana Saleem who continuously motivated me, Rabeeah Ali for her support, Arslan and Noman for help in data collection, my husband, mother in law, mom and my entire family for their continuous support in all the matters.

Lastly but most importantly my biggest motivation was the never ending efforts of my beloved son, who wakes up daily and tirelessly challenges himself to learn new things. His giggles and love made me come so far.

Contents

| | | |
|----------|--|----------|
| 1 | Introduction | 1 |
| 1.1 | Motivation | 2 |
| 1.2 | Problem Statement | 3 |
| 1.3 | Objective and Scope of Thesis | 3 |
| 1.4 | Structure of Thesis | 4 |
| 2 | VISUAL FIELD TESTS | 5 |
| 2.1 | Anatomy of Human Eye | 5 |
| 2.2 | Structure of Retina | 6 |
| 2.3 | Aspects of Vision | 8 |
| 2.4 | Visual Pathways: How Our Eyes See | 10 |
| 2.5 | Glaucoma | 12 |
| 2.6 | Diagnostic Techniques for Glaucoma | 13 |
| 2.7 | Visual Field | 13 |
| 2.8 | Perimetry | 15 |
| 2.8.1 | Decibels | 16 |
| 2.8.2 | Static Perimetry | 17 |
| 2.8.3 | Testing Algorithms | 18 |
| 2.9 | Humphrey Visual Field Tests | 21 |
| 2.9.1 | Humphrey Visual Field Analyzer | 21 |

| | | |
|----------|--|-----------|
| 2.9.2 | Interpreting Humphrey Visual Field Reports | 22 |
| 3 | LITERATURE REVIEW | 26 |
| 3.1 | Glaucoma : The Optic Neuropathy | 26 |
| 3.2 | Standard Automated Perimetry | 27 |
| 3.3 | Scoring Glaucoma | 31 |
| 4 | METHODOLOGY | 36 |
| 4.1 | Extraction of Region of Interest | 36 |
| 4.1.1 | Extraction of Green Channel | 37 |
| 4.1.2 | Binarizing the Cropped Image | 38 |
| 4.1.3 | Connected Component Analysis | 40 |
| 4.1.4 | Removal of Axes | 40 |
| 4.2 | PKS extraction | 40 |
| 4.3 | PKS labeling | 41 |
| 4.4 | Overall PKS count and Quantitative Score | 50 |
| 4.5 | Count of PKSs per ISNT Region | 52 |
| 5 | EXPERIMENTAL RESULTS | 55 |
| 5.1 | Dataset Description | 55 |
| 5.2 | PKS Extraction | 57 |
| 5.3 | PKS Classification | 57 |
| 5.4 | Mapping of SCHEIE Scores to Grades | 58 |
| 6 | CONCLUSION AND FUTURE WORK | 62 |
| 6.1 | Conclusion | 62 |
| 6.2 | Contribution | 63 |
| 6.3 | Future Work | 63 |

List of Figures

| | | |
|------|--|----|
| 1.1 | Spatial Extent of the Monocular Visual Field[1] | 1 |
| 1.2 | Spatial Extent of the Binocular Visual Field[1] | 2 |
| 1.3 | Illustration of vision with Glaucoma[6] | 3 |
| 2.1 | Anatomy of Human Eye[7] | 6 |
| 2.2 | Organization of Retinal Cells[8] | 7 |
| 2.3 | Highest Acuity is at Fovea [9] | 9 |
| 2.4 | Visual Pathway (Top View)[10] | 10 |
| 2.5 | Visual Cortex[11] | 11 |
| 2.6 | Visual Field Illustration as Hill of Vision[12] | 13 |
| 2.7 | Visual Field Boundary[13] | 14 |
| 2.8 | Fovea is located at the fixation i.e. zero degrees[12] | 14 |
| 2.9 | Generalized Loss of Sensitivity[12] | 15 |
| 2.10 | Focal Loss[12] | 15 |
| 2.11 | Frequency of seeing curve[13] | 17 |
| 2.12 | Full threshold bracketing strategy[14] | 18 |
| 2.13 | Testing 76 test locations[15] | 19 |
| 2.14 | Testing 54 locations[14] | 20 |
| 2.15 | Measuring central field only[15] | 20 |
| 2.16 | Humphrey Visual Field Analyzer[14] | 21 |
| 2.17 | Goldman sizes for stimuli [16] | 22 |

LIST OF FIGURES

| | | |
|------|--|----|
| 2.18 | Humphrey Visual Field Test Report Pattern[14] | 23 |
| 3.1 | Comparison between Full Threshold, SITA Standard and SITA Fast [24] | 28 |
| 3.2 | Total 65 sectors were obtained: 38 sectors from 30-2 and 29 sectors from 10-2 visual fields[26]] | 29 |
| 3.3 | 10-2 visual field is affected in early glaucoma as well [28]] | 30 |
| 3.4 | PSD,MD and VFI according to staging systems AGIS, GSS [36] | 33 |
| 4.1 | Block Diagram of Proposed Methodology | 37 |
| 4.2 | Original HVFT Report Imported into MATLAB with the ROI highlighted | 38 |
| 4.3 | ROI Extraction from the entire HVFT Report (a): Input Image (b): Otsu's segmentation (c): Row sum vector and column sum vector and minR, minV extraction (d): Extracted ROI centered at $\text{Img}(\text{minR}, \text{minV})$ | 38 |
| 4.4 | Extracted Green Channel | 39 |
| 4.5 | Inverted Binary Image | 39 |
| 4.6 | Connected components in image processing having pixels connected by their faces (4-connectivity), or by their faces and edges (8-connectivity) [38] | 40 |
| 4.7 | Figure containing only the key elements extracted | 41 |
| 4.8 | Single and Four dots combined | 43 |
| 4.9 | 87 distinct objects detected | 43 |
| 4.10 | Clustered four dots using isotropic dilation | 44 |
| 4.11 | Probability less than 5 percent points segmented | 44 |
| 4.12 | Three largest blob PKS | 45 |
| 4.13 | Probability less than 0.5 percent points segmented | 46 |
| 4.14 | Probability less than 2 and 1 percent points | 46 |
| 4.15 | Probability less than 1 percent points segregated | 47 |
| 4.16 | Result of first image subtraction | 47 |
| 4.17 | Result of second image subtraction | 48 |

LIST OF FIGURES

| | | |
|------|---|----|
| 4.18 | Result of third image subtraction | 48 |
| 4.19 | Clustered single dots and probability less than 2 percent points | 49 |
| 4.20 | Single dots segregated | 49 |
| 4.21 | Probability less than 2 percent points segregated | 50 |
| 4.22 | SCHEIE Rules for scoring Glaucoma | 51 |
| 4.23 | Superior and Inferior Hemifields scored according to SCHEIE method | 52 |
| 4.24 | Inferior, Superior, Nasal ,Temporal and Central Regions in Optometry[42] | 52 |
| 4.25 | Division of PD into 6 Regions | 53 |
| 4.26 | Superimposing 6 Regions onto VFT Report | 53 |
| 4.27 | Calculation of SCHEIE scores for 4 ISNT regions | 54 |
| 4.28 | Calculation of SCHEIE scores for 6 regions | 54 |
| 5.1 | (a): Normal Eye (b): Early Glaucoma (c): Severe Glaucoma | 56 |
| 5.2 | Ground Truth for Image 14 | 58 |
| 5.3 | Falsely Detected $P < 0.5\%$ for Image 14 | 59 |
| 5.4 | Few cases of graded Normal VFs having no glaucoma | 60 |
| 5.5 | Examples of graded VFs showing early glaucoma with individual SCHEIE Scores in all 6 regions | 60 |
| 5.6 | Examples of graded VFs showing moderate glaucoma with individual SCHEIE Scores in all 6 regions | 61 |
| 5.7 | Examples of graded VFs showing advanced glaucoma with individual SCHEIE Scores in all 6 regions | 61 |

List of Tables

| | | |
|-----|--|----|
| 2.1 | Comparison of Categories of Glaucoma[11] | 12 |
| 2.2 | Diagnostic tests for Glaucoma[12] | 13 |
| 2.3 | Information about Visual Fields from MD and PSD[16] | 24 |
| 3.1 | Hodapp Parrish Anderson Staging System[31] | 34 |
| 3.2 | The Field Damage Likelihood Score [32] | 35 |
| 3.3 | DATASET BY RASKER, MARGA TE, ET AL [33] | 35 |
| 4.1 | Overall count of each PKS segregated and classified | 50 |
| 4.2 | Count and scoring of PKS in the overall image according to SCHEIE criterion | 51 |
| 5.1 | Dataset Used | 56 |
| 5.2 | Mean and Standard Deviation of Statistical Features Used for PKS Seg- mentation | 57 |

List of Abbreviations and Symbols

Abbreviations

| | |
|-------------|-------------------------------------|
| PKS | Probability Key Symbol |
| QoL | Quality of Life |
| HVFT | Humphrey Visual Field Test |
| ISNT | Inferior, Superior, Nasal, Temporal |
| SAP | Standard Automated Perimetry |

CHAPTER 1

Introduction

The visual field area of the person is described as the boundaries of the area in which a person can see for a certain moment while viewing at a fixed direction; without moving his eyes or head and beyond which nothing can be viewed. The extent of visual field of healthy human eye is constant and is important to consider as the narrowing of the visual field negatively effects one's daily life activities and hence quality of life (QOL). There are two types of visual fields : monocular and binocular. The visual field of one eye is called monocular visual field.

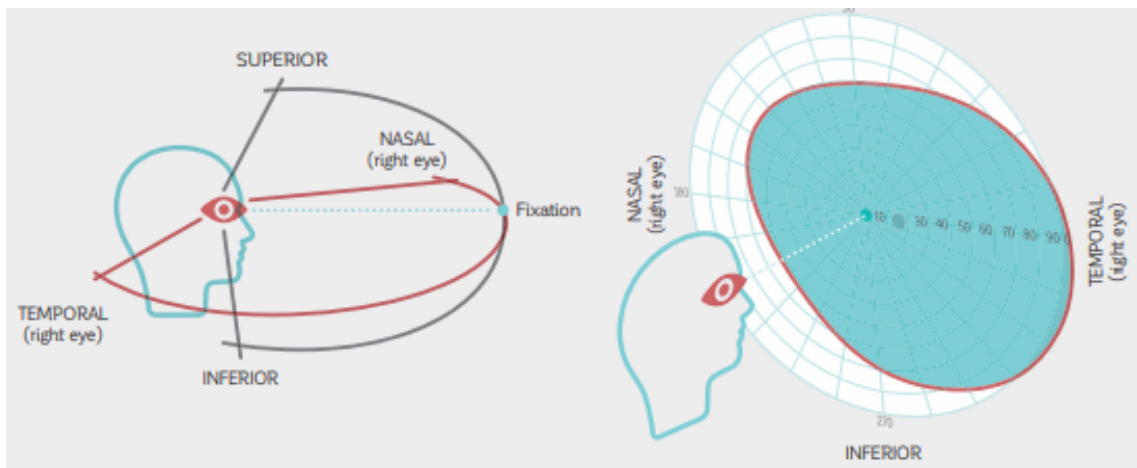


Figure 1.1: Spatial Extent of the Monocular Visual Field[1]

The facial anatomy of the person (brows, eyes, cheeks) limit the spatial extent of the monocular visual field in normal eyes. Spatially; the monocular visual field extends from approximately 60 degrees nasally to 90 degrees temporally and from 60 degrees

superiorly to 70 degrees inferiorly[3].

The binocular visual field contains input integration and mapping information from both the eyes defining the visual acuity and depth of perception. The overlapping region of central 60 degrees comprises of binocular visual field. [1]

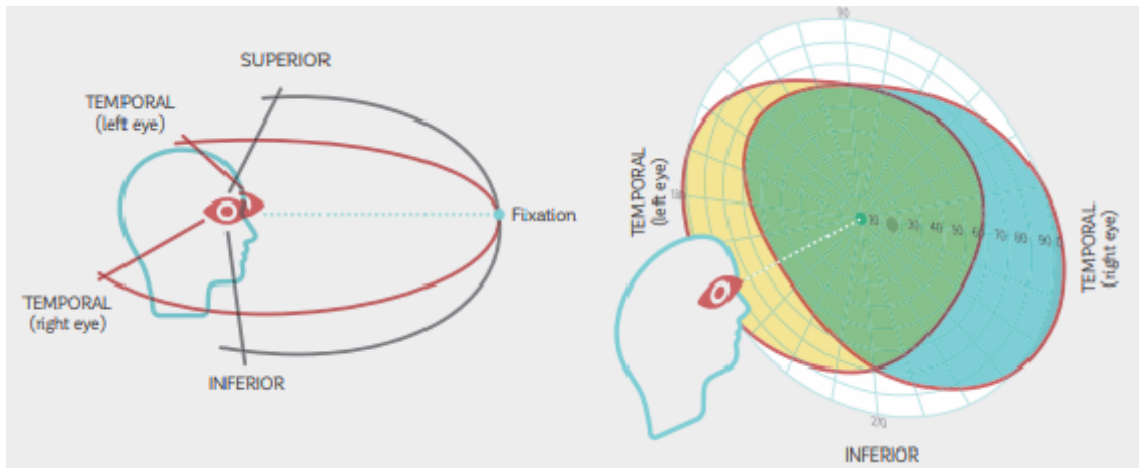


Figure 1.2: Spatial Extent of the Binocular Visual Field[1]

Glaucoma is a general term including a range of ocular conditions that cause a specific neuropathy of the optic nerve[1].After cataracts, glaucoma is the second leading cause of blindness in the world and can occur in all age groups but is most common in the elderly[2]. Glaucoma produces a characteristic progressive damage to the optic nerve resulting in the loss of the visual function loss[3]. The most common clinical method of measuring the function of the visual system is perimetry or visual field testing which assesses the eye's ability to detect the brightness of small points of light projected in both the central and peripheral areas of vision [4].The detection of an impairment in the visual field due to glaucoma represents the location and extent of optic nerve damage. Standard automated perimetry (SAP) is currently the gold standard for detecting glaucomatous visual field loss clinically worldwide[5].

1.1 Motivation

There has been very little work done in the past on the quantitative analysis of Humphrey Visual Field (HVF) reports. The report contains statistical plots of total deviation and



Figure 1.3: Illustration of vision with Glaucoma[6]

pattern deviation which display the probability key symbols (PKSs) in the ISNT quadrant for each patient. The count and location of each of these PKS has its significance as the individual and overall count of PKS helps to determine the extent of glaucoma and the location of PKS helps to determine the characteristic pattern of glaucomatous damage to the visual field of patient. Currently there is no algorithm to automatically segment, count and locate the PKSs in the HVF reports. This short coming has motivated me towards the development of an algorithm in MATLAB R2017 Image Processing Toolbox which will be the first of its kind. Therefore, we aim to extract, count and locate the PKSs accurately which will aid the ophthalmologists in their diagnosis.

1.2 Problem Statement

Visual field test is performed to analyze effect of Glaucoma on patient's vision. Traditionally manual analysis of report is being done which requires expertise. In this research, we aim to use image processing and decision support techniques for automated analysis of VFT reports to grade Glaucoma level.

1.3 Objective and Scope of Thesis

It is really essential to detect and treat (mostly asymptomatic) glaucoma as early as possible to avoid the risk of blindness. The objectives of the thesis are as follows:

- To segment out the ROI from the rest of the image
- To label each of the PKS as one of the five categories

- To determine the location PKs in the ISNT quadrants
- To grade Glaucoma

Since glaucoma is a very common illness, a large number of patients present in front of the doctors. Hitherto, there is no other way to assist doctors in the analysis of visual field reports. Our aim is to assist the ophthalmologists in reaching the conclusion about glaucoma extent of patients by analyzing the statistical values generated in the report, since glaucoma presents characteristic damages in the optic nerve.

1.4 Structure of Thesis

Remaining part of the thesis is organized as follows:

Chapter 2 discusses the anatomy and physiology of human eye emphasizing on the underlying mechanism of functioning of visual pathways as well as retinal structure and function (imaging) and components of vision. It discusses the structural and functional damage caused by glaucoma; and the perimetry in detail explaining the testing strategies, the measurement units and the perimeter used to measure visual fields. It also discusses in detail the Humphrey visual field analyzer and the interpretation of visual field reports.

Chapter 3 discusses the literature searched on three main topics: firstly recent studies conducted to investigate the developments in the causes, risk factors and structural damages in the study of Glaucoma, secondly the chronological adaptation of various algorithms used in the standard automated perimetry (SAP) and thirdly the different scoring methods used by the clinicians in the world to grade glaucoma.

Chapter 4 discusses in detail the implemented methodology with the explanation of each module.

The explanation of databases used for evaluation purposes is given in **Chapter 5** including all the experimental results are discussed in detail with all desired figures and tables.

Chapter 6 concludes the thesis and reveals future work of proposed system.

CHAPTER 2

VISUAL FIELD TESTS

2.1 Anatomy of Human Eye

Eye is one of the most complex organ of human body and consists of three separate layers. The formation of these three ocular layers is as follows:

- Outer Layer is made up of sclera and cornea
- Middle Layer is made up of iris, ciliary body and choroid
- Inner Layer comprises of retina.

These three layers surround the transparent structures of aqueous, vitreous and the lens. The tough outer coat that protects the entire eye ball is known as sclera. The front portion of the eye which is convex in shape and bulges outside is cornea through which light enters the eye. Located just behind the cornea is a dark muscular diaphragm known as iris containing a hole in the middle called pupil. The function of the iris is to regulate the amount of light entering the eye by adjusting the size of pupil.

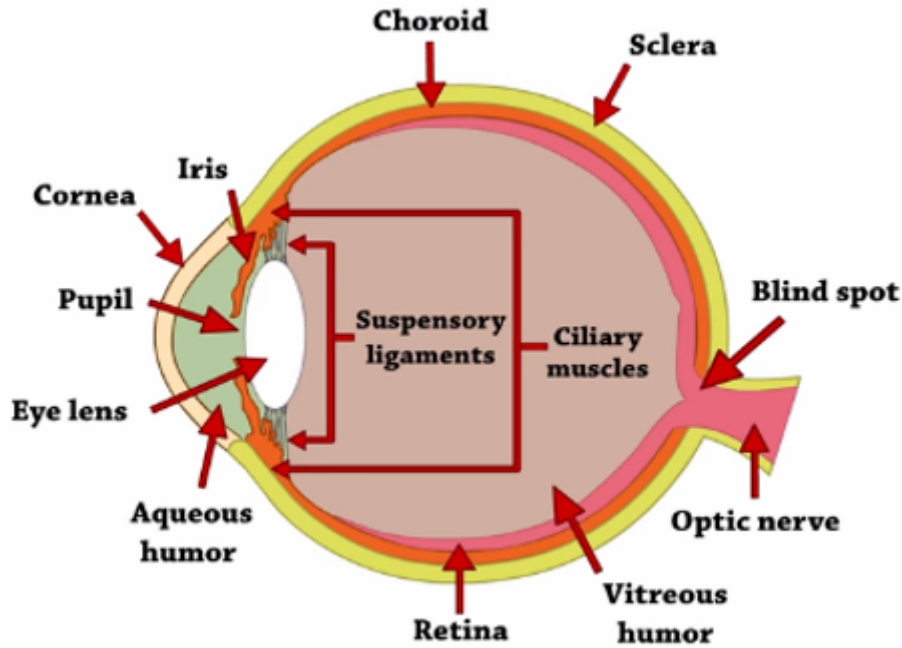


Figure 2.1: Anatomy of Human Eye[7]

Figure 2.1 shows the anatomy of the human eye. The ciliary muscles and the suspensory ligaments (ciliary zonules) keep the lens in its place by providing supporting to it. They also adjust the focal length of the eye to help view nearby and distant objects clearly. The area between the cornea and eye lens is filled by a viscous liquid called aqueous humor. It prevents the eye from collapsing due to changes in the atmospheric pressure. Retina is a delicate membrane having a large number of light sensitive cells. Choroid is the vascular layer of the eye containing blood vessels that nourish the inner parts of the eye. Retina is the light sensitive region of the eye. The optic nerve carries impulses from eye (retina) to the brain which interprets them as an image.

2.2 Structure of Retina

On the basis of class type; the retinal neuron cells are divided into six categories: photoreceptors, bipolar cells, horizontal cells, amacrine cells, ganglion cells and Mullerian glia. The axons of the ganglion cells exit the eye to form optic nerve head (ONH) also known as Optic Disc (OD). There are no photoreceptor cells (rods or cones) at the ONH hence creating a natural blind spot in each eye at this location also called physiological scotoma. It is typically located 15° temporally and $1-2^\circ$ inferiorly to the fovea, and its

size is approximately 5° horizontally and 7° vertically. We do not notice the presence of natural blind spot in our eyes because the central field of vision of both our eyes overlaps and also because our brain fills in for the incomplete information[8] .

The axons of the ganglion cells make the optic nerve. The inner most layer of the retina which is nearest to the eye comprises of ganglion cells. The photoreceptor cells of rods and cones are located in the outermost layer of retina. They absorb the light which reaches retina and use the process of phototransduction to convert the absorbed light to electric signals. There are approximately 105 million photoreceptors and 1.2 to 1.5 million ganglion cells in the human retina. Figure 2.2 shows the organization of the retinal cells.

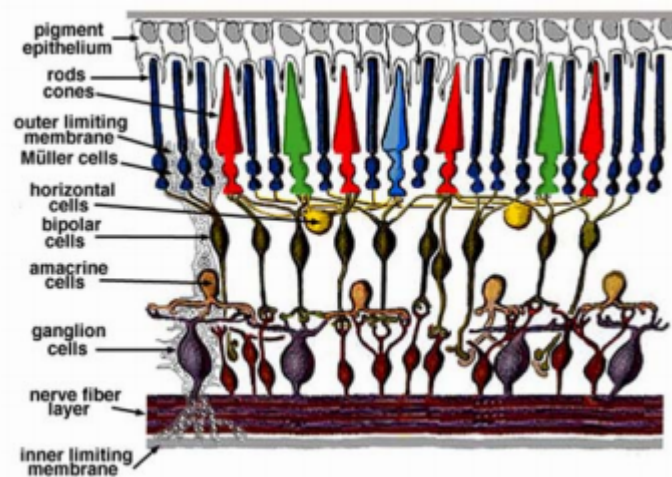


Figure 2.2: Organization of Retinal Cells[8]

The rods work under scotopic conditions and cones work under photopic conditions and are responsible for colored RGB vision hence responding to three different intensities of red, green and blue wavelengths. These rods and cones are unevenly distributed throughout the retina. The ganglion cells are of three types: Parvocellular, Magnocellular and Koniocellular ganglion cells. The Parvocellular make up the 80 percent of the ganglion cells and work slowly; with detail resulting in object recognition and form representation.

The magnocellular cells work quickly but follow less detail and are responsible for object localization and motion. They make up 10 percent of the ganglion cells. The Koniocellular cells operate at moderate speed and result in colored vision comprising of the remaining 10 percent of the ganglion cells.

The dip in the retinal membrane is called fovea which contains a large concentration of cones. Rods on the other hand are located near the periphery of the eye. The reason of the dip of the fovea is the fact that photoreceptors are connected to other neurons that send axons through the optic nerve into the brain. Hence when light hits the fovea, more light falls on cones rather than being absorbed by axons in its way; hence giving higher resolution. The image of the object is formed on the fovea which is responsible for sharp central vision comprising of more detail.

2.3 Aspects of Vision

The following are the aspects of the vision.

- Visual Acuity
- Colored Vision
- Scotopic Vision/Adaptation to darkness
- Accomodation
- Sensitivity to contrast
- Sterioscopic Vision

Let's explain them briefly one by one.

Visual acuity is defined as the “spatial resolving capacity” of the eye or, in other words, the size of an object that can be resolved with an eye. Visual function is most commonly tested by visual acuity since this test is very easy to perform and uses very simple equipment i.e it is tested by using specific eye charts clinically[9]. Fovea is the region of highest acuity as shown in figure 2.3.

Light perception occurs in retina via cones which are of three types corresponding to three types of colors: red, green and blue. Upon visualizing a color, each cone sends its own distinct signal to the brain. For example upon viewing the yellow light, both the red and green cones get activated sending signals to the brain. The brain hence detects the color as yellow. Human eye can not view colors in dark as the rods which take over

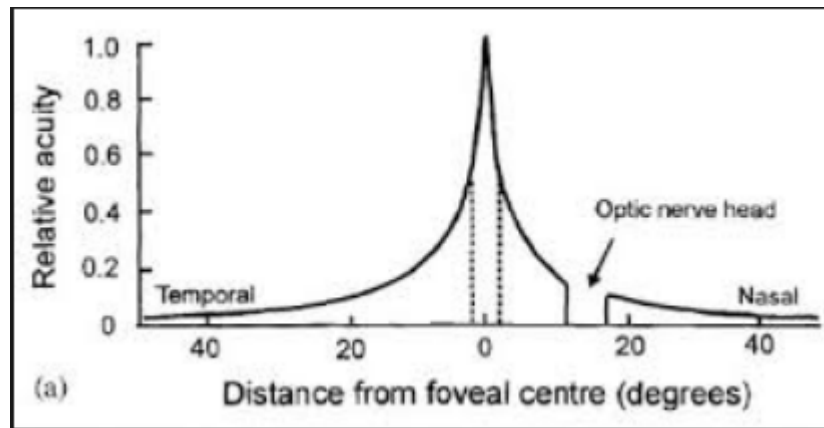


Figure 2.3: Highest Acuity is at Fovea [9]

in darkness are only of one type; therefore sending only one type of signal to the brain. That is they either send 1 or 0 to the brain meaning light or no light.

Accommodation reflex comprises of three functions of the eye: convergence, pupillary constriction and rounding of the lens. When an object approaches eyes; both the eyes converge to focus the image on the fovea. Inappropriate convergence leads to double vision or diplopia. The pupil constricts enough to regulate the light refracted by the lens and reflected the object failing which the object might appear blurred. Finally the lens round up according to the distance of the object so that image of the near or distant object falls on retina. All these three phenomenon of convergence, pupillary constriction and rounding of the lens combine to perform accommodation.

Unlike visual acuity which tests the ability to measure smaller and smaller objects; contrast sensitivity is used to measure the ability to distinguish increments of darkness versus light. e.g. vision in fog. It is very important especially while driving at night.

Human eyes perceive the concept of depth by combining the two images from the left and right eye hence enabling us to have a 3-dimensional vision. This process is called Stereopsis and the vision is called Stereoscopic Vision.

2.4 Visual Pathways: How Our Eyes See

The visual pathway as shown in figure 2.4 begins at our eyes. An object is simultaneously viewed by both our eyes: left and right. The image of the object is formed at the retina of both of the eyes. The photoreceptor cells of the retina excite the bipolar cells; which in turn synapse with the ganglion cells. The axons of the ganglion cells exiting the eye; form the optic nerve. It is very important to note that the myelin sheath of the ganglion cells is secreted/formed by oligodendrocytes; hence ganglion cells though originating from eye (sensory organ which is not a part of brain or central nervous system) are considered the part of central nervous system (brain and spinal cord). The optic nerve (formed by axons of ganglion cells) is a sensory nerve and does not contain any motor organs meaning it just carries impulses from eyes to brain and vice versa.

The left side of the retina in each eye receives light from left visual field and the right side of retina receives light from right visual field. The optic nerve originating from retina of each eye contains two components: nasal (close to nose) and temporal (close to ears/temples). A few millimeters behind the optic nerve head redistribution of the

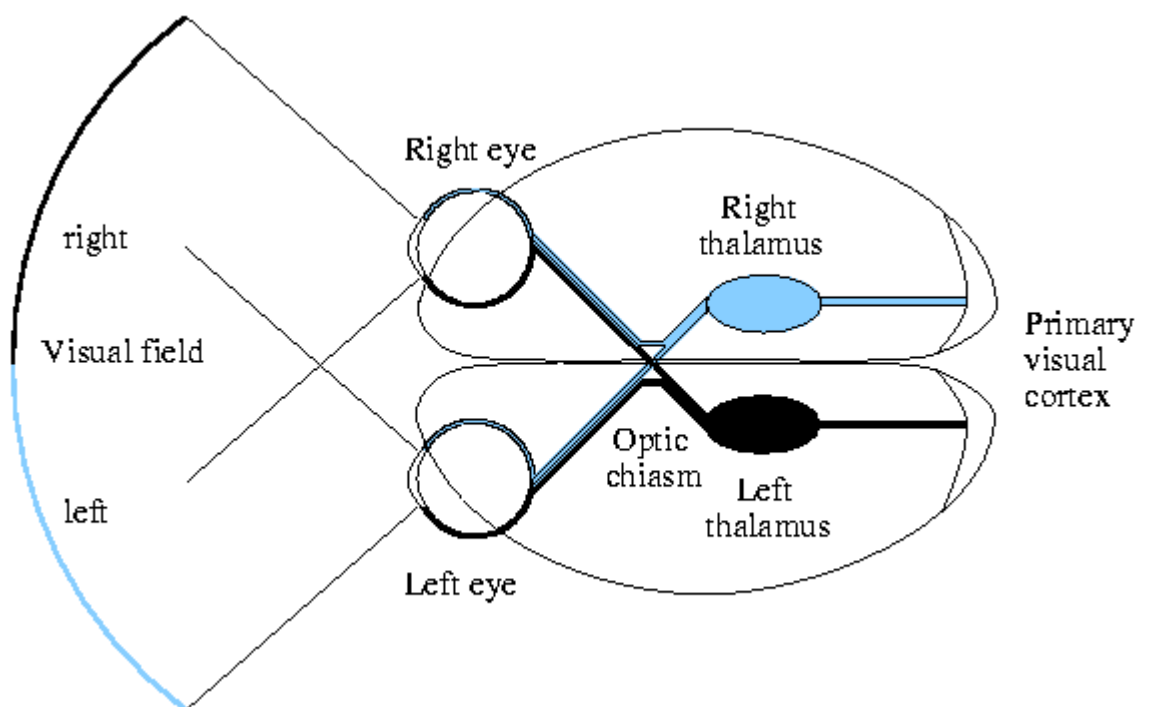


Figure 2.4: Visual Pathway (Top View)[10]

axons take place. The nasal component of left and right eye cross over at the part of brain called optic chiasm. Whereas the temporal components of the left and right optic nerve pass as such. This crossing over at the optic chiasm is the reason that our eye balls move simultaneously to the sides. Also, due to this optic chiasm we are able to see a large portion of visual field with only one eye even if our other eye is covered. After crossover, the temporal and nasal halves of left eye form left optic track and temporal and nasal component of right eye form right optic track. Hence at the chiasm the fibers decussate so that beyond the chiasm all of the fibers for the right hand are now in the left visual pathway and the fibers for the left hand are in the right visual track. Until now we have covered the prechiasmatic pathway. Figure 2.5 shows the visual cortex in the brain.

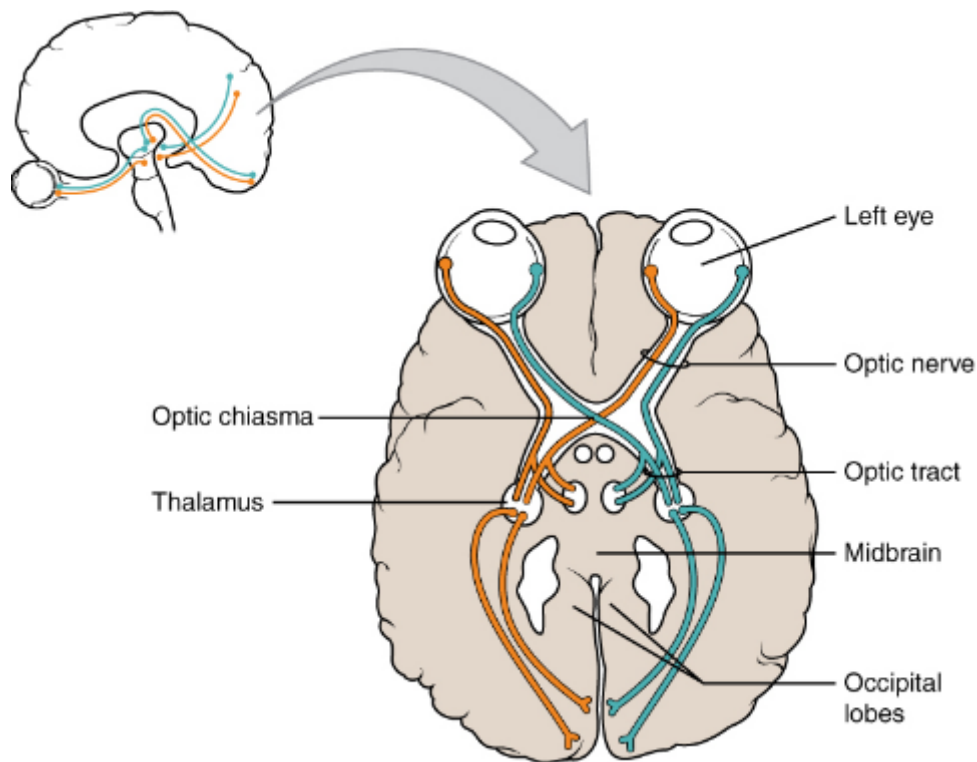


Figure 2.5: Visual Cortex[11]

Let us go beyond to discuss retro chiasmatic track which is made up of optic track, lateral geniculate body, optic radiations and occipital lobes. The right and left optic tracks connect to the lateral geniculate nucleus of the thalamus. Every signal before going to brain is relayed in the thalamus. The fibers of thalamus then extend to the cortex of the brain. The primary visual area lies in the occipital lobe of the cortex. The image

is thus received in the primary visual area of occipital lobe and is relayed to secondary visual area of the occipital lobe for further analysis. The image formed on the retina was an inverted image but the image is received in its proper orientation in the occipital lobe in the brain.

2.5 Glaucoma

Glaucoma is an ocular disease that may result in permanent loss of eyesight if not detected and treated at an early stage. Eye produces a fluid called aqueous humor that originates behind the iris and drains through a tabular meshwork after floating in the front portion of the eye. It maintains a balanced pressure called Intraocular Pressure (IOP) inside the eye and keeps the eye inflated. However, if drainage route is blocked; the fluid builds an abnormal IOP which may cause damage of the optic nerve which cannot be reversed and leads to permanent blindness i.e. glaucoma. According to the World Health Organization (WHO) glaucoma is the second major cause of blindness in the world.

Glaucoma has no early symptoms or pain and is also known as the “silent thief of the sight” [3]. Therefore, for diagnosing glaucoma there are several techniques such as measuring IOP, Cup to Disc Ratio (CDR) calculation using Fundus Images, use of Optical Coherence Tomography (OCT) for thickness calculation of Retinal Nerve Fiber Layer (RNFL) and Visual Field Tests (VFT).Based on causes and symptoms, glaucoma is categorized into main two types as shown in table 2.1

Table 2.1: Comparison of Categories of Glaucoma[11]

| Open-angle Glaucoma | Angle-closure Glaucoma |
|---------------------------------------|---------------------------------------|
| Caused by clogging of drainage canals | Caused by blockage of draining canals |
| Has slow progression | Develops quickly |
| Irreversible | Needs immediate medical treatment |
| No noticeable symptoms | Has noticeable symptoms |

2.6 Diagnostic Techniques for Glaucoma

The following table 2.2 enlists the examination quantity and the test used to measure that parameter.

Table 2.2: Diagnostic tests for Glaucoma[12]

| Examination parameter | Name of Test |
|---|-----------------------------------|
| The inner eye pressure | Tonometry |
| Shape and color of optic nerve | Ophthalmoscopy (dilated eye exam) |
| The complete field of vision | Perimetry (Visual field test) |
| The angle in the eyes where iris meets cornea | Gonioscopy |
| Thickness of cornea | Pachymetry |

2.7 Visual Field

Dr. Harry Traquair, a Scottish scientist has famously described field of vision as "island hill of vision in a sea of darkness" as shown in figure 2.6

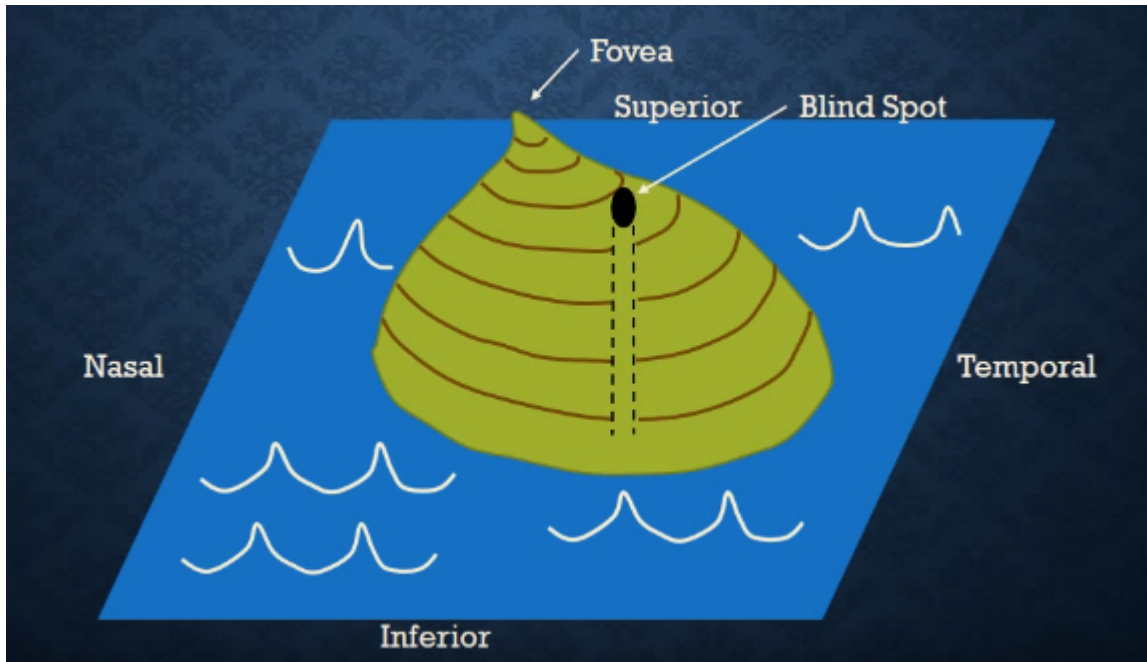


Figure 2.6: Visual Field Illustration as Hill of Vision[12]

CHAPTER 2: VISUAL FIELD TESTS

The shape of the island represents differences in sensitivities of different regions of the retina. Isopters represent the regions having similar sensitivities. The coordinate system used in visual fields is Inferior, Superior, Nasal, Temporal (ISNT). The highest peak of the island of field of vision has the highest sensitivity and corresponds to fovea. The area in which there is zero sensitivity is defined as blind spot and this is the area of absolute scotoma meaning even if you shine the brightest light on it; nothing will be seen by it. It is about 7-8 degrees in vertical diameter and 5 to 6 degrees in horizontal diameter and is approximately 1.5 degrees below the horizontal midline. The following figure 2.7 illustrates the visual field boundary.

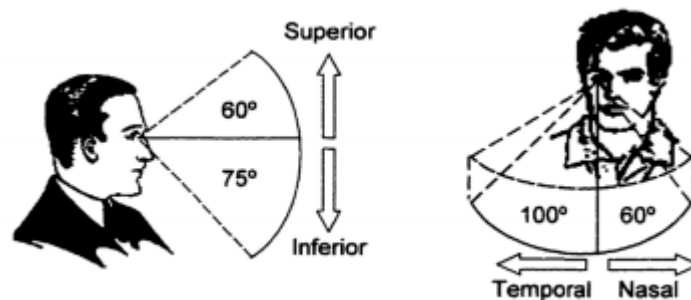


Figure 2.7: Visual Field Boundary[13]

In visual field zero degrees corresponds to fovea and is always set at the fixation as shown in figure 2.8.

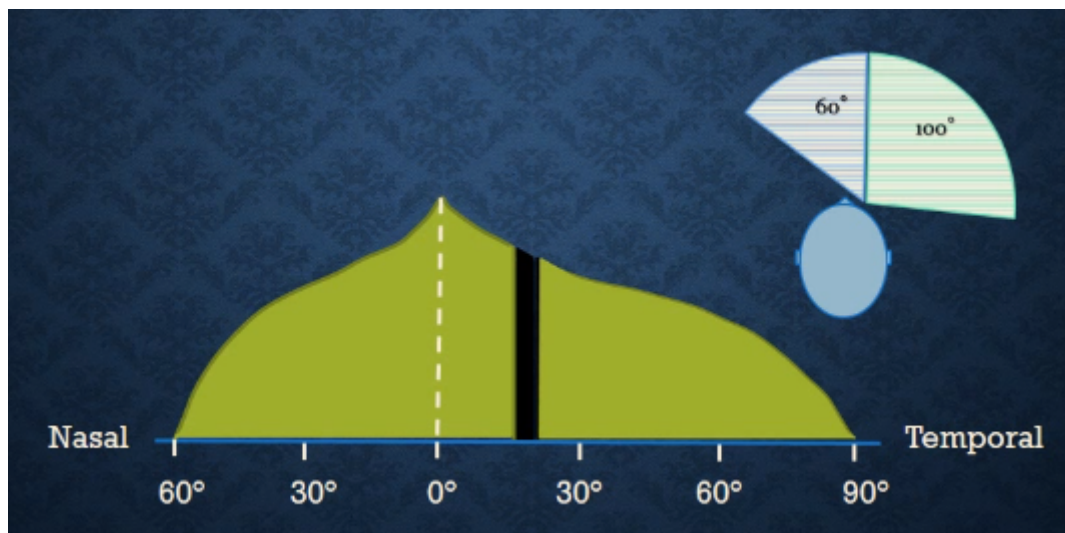


Figure 2.8: Fovea is located at the fixation i.e. zero degrees[12]

Any change in the shape or height of the hill of vision points to underlying pathologies.

If the height of the hill of vision is less as compared to what it should be for patients of that age; but this loss is equal at all points then this is called "generalized loss of sensitivity" and can be due to old age or some disease as shown in figure 2.9.

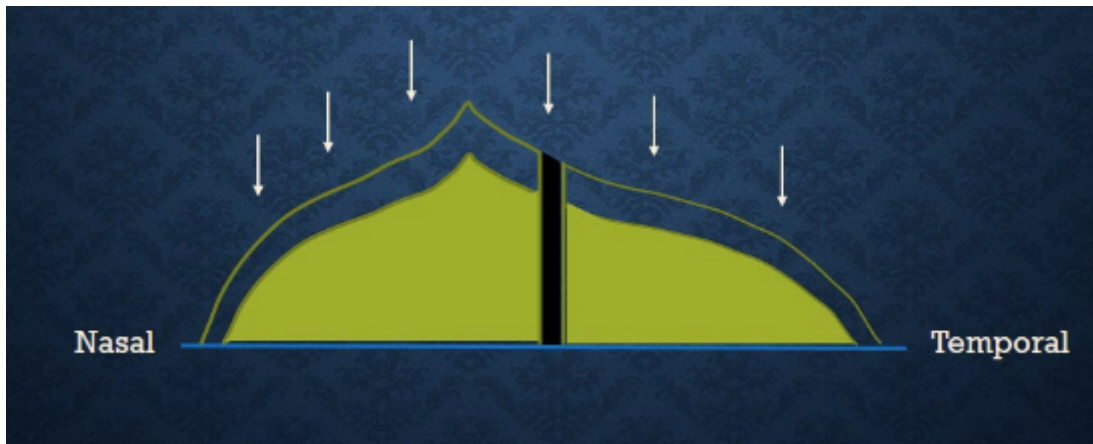


Figure 2.9: Generalized Loss of Sensitivity[12]

Contrary to generalized losses the focal losses are like pits on the hill of island. They represent the creation of scotomas (e.g. due to glaucoma) in the field of vision of the person. In glaucoma the creation of scotomas follows a specific pattern as shown in figure 2.10.

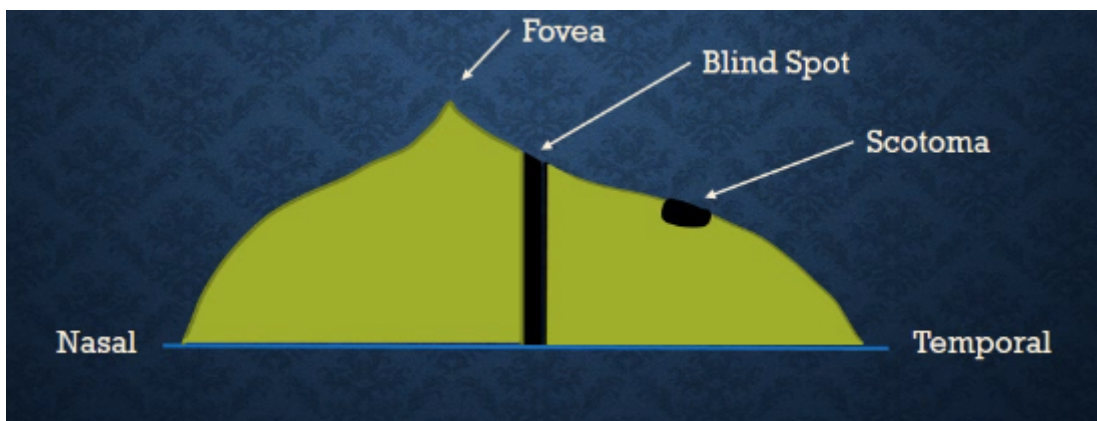


Figure 2.10: Focal Loss[12]

2.8 Perimetry

Glaucoma causes functional and structural damage. The functional damage can only be quantified by measuring the visual field of the patient. Perimetry is the science

of measuring the visual field of the patient using a perimeter (device specified for the purpose of mapping visual field). Perimetry is also used to measure the progression of the damage to the visual field of the patient over the course of time and is the direct measure of the damage caused by glaucoma as opposed to IOP which gives us an indirect measure. It helps to determine the disease and the location of lesions because diseases specifically Glaucoma and other lesions produce characteristic patterns of loss in the visual field. Perimetry also helps to specify the extent of loss and monitor its progression. Though perimetry is specifically used for Glaucoma but any disease in the visual (ocular) pathway presents its affect on the visual field. In addition to the measuring the extent of the visual field of a patient it is important to measure the sensitivity of the patient to the light intensity. The intensity of light is inversely related to the sensitivity. A person who can see in a very dim light has a very high light sensitivity and vice versa. Under normal day light conditions; the sensitivity of healthy eyes is highest at the center of the hill of vision and decreases at the edges of the hill.

Perimetry helps to quantify a patient's sensitivity of light. Different stimuli of varying intensities are presented to the patient at various locations who fixates one eye at a time at a certain point and hence the test measure the ability of the eye to distinguish differences in the luminance. Stimuli are presented on a surface and the luminance is measured as the light per unit area reflected from the screen into the eye. Units of luminance are apostilbs (asb) or candela per square meter (cd/m^2) and represent light flux per unit area.

The frequency of seeing curve gives us the probability of perception of a stimulus versus stimulus intensity. The curve tells that there is a very probability of viewing a highly intense stimulus and a very low probability of viewing a low intensity stimulus at a specific point. This is depicted by flat curves along the ends of x-axis. However, the curve between these two extremities is quite steep and the range of intensities for a trained observer at which they may or may not perceive the stimulus spans roughly 3 dB as shown in figure 2.11.

2.8.1 Decibels

Under normal day light conditions, the human eye can adapt to a large range of luminance from 0 to 10,000 apostilbs which is impossible to be displayed . An inverse

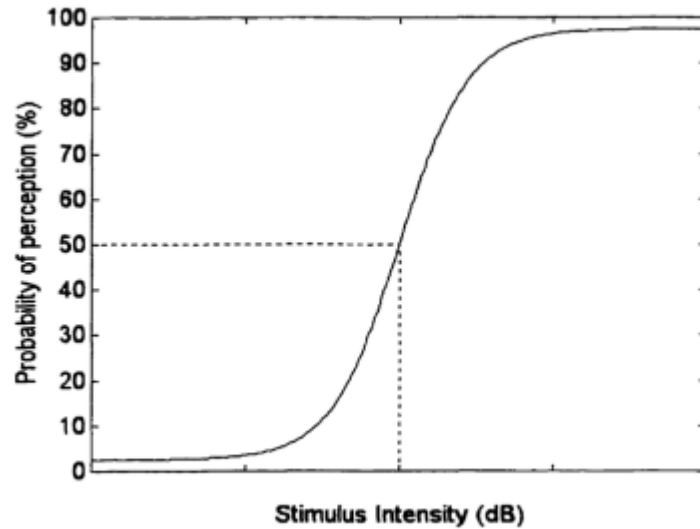


Figure 2.11: Frequency of seeing curve[13]

relation occurs between sensitivity and luminance. Also, the sensitivity does not change linearly with luminance in apostilbs hence to resolve all these issues an intuitive scale of decibels is used in perimetry. The value of db scale lies in the range of 0 to 32 db where a value of 0db means that the patient was unable to see the brightest stimulus and 32 db represents normal vision of fovea for healthy eye.

2.8.2 Static Perimetry

The two most common types of perimetry are kinetic and static and they differ on the basis of mobility of stimulus. In the case of kinetic perimetry the stimulus moves however in the case of static perimetry the size and location of the target remain constant.. The static perimetry is further divided into standard automated perimetry (SAP) and selective perimetry. Today the worldwide accepted standard of perimetry is SAP and we will be further discussing it in detail.

Standard Automated Perimetry

With the advent of computers; the manual perimetry is replaced by automated perimetry. The patient does not know where the next stimulus would be hence improving the fixation and reliability of the test.

2.8.3 Testing Algorithms

Lets explain the testing algorithms in detail.

Full Threshold

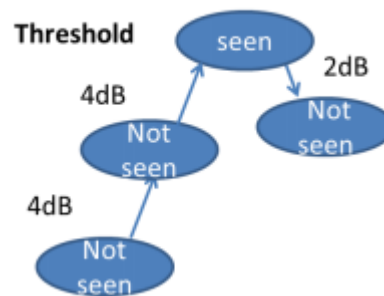


Figure 2.12: Full threshold bracketing strategy[14]

As shown in figure 2.12 ; initially full threshold algorithm was used in which a stimulus is presented at a test location. The threshold is determined at every point in the visual field using 4-2 bracketing algorithm. The stimulus intensity is varied so that threshold is crossed twice, first using 4-db steps and then 2-db steps. The stimulus intensity was decreased by 4 db. Threshold is either the intensity of the last seen stimulus (HFA) or the average of the last seen and unseen stimulus (Octopus). It is most accurate however most time consuming hence it is not suitable for all patients.

SITA: Standard and Fast

SITA stands for Swedish Interactive threshold algorithm and is designed to decrease the test time by incorporating the patient's responses in real time in an intelligent way; hence reducing the time for test as compared to full threshold strategies and not compromising on reliability and accuracy. SITA is most widely used algorithm especially for Humphrey Visual Field Analyzers. There are two versions of SITA: SITA Standard and SITA Fast. SITA uses Bayesian model to predict the information about location and intensity of future stimuli. By inculcating the information about the neighborhood the stimuli which are unlikely to be seen or the stimuli that have a very high probability to be seen are excluded from exhaustive research. SITA standard tests 90 percent of

the test locations and exits if it reaches a definite result. Similarly, SITA Fast exits if on testing 80 percent of the test locations a result is reached. SITA standard takes approximately 7 minutes per eye and SITA fast takes approximately 4 minutes per eye.

30-2, 24-2, 10-2

The first part of the name indicates the extent to which the visual field is being tested i.e. 30 means the visual field extending 30 degrees both to left and right from the center is being tested. Hence in effect a total of 60 degrees of visual field is being tested. Similarly, 24 and 10 refers to extension of visual field test to 24 degrees and 10 degrees in both directions from the center respectively. Coming to second part of the name, the 2 represents the second standard developed to present stimuli. Initially, 30-1 standard was introduced in which the initial stimulus was located directly on x and y axis and the difference between next stimuli from the previous was 6 degrees. Whereas in 30-2, no stimuli are presented on the vertical and horizontal axis and the distance of stimuli from vertical axis is 3 degrees.

Both SITA Standard and Fast follow one of the three types of tests: 30-2, 24-2 or 10-2. 30-2 and 24-2 are same except the most outer ring. 30-2 has 76 test locations whereas 24-2 has 54 test locations. The distance between any test location and the next one is 6 degrees as shown in figure 2.13

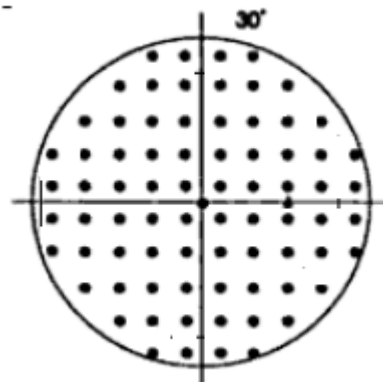


Figure 2.13: Testing 76 test locations[15]

The distance between the vertical line and first test location is 3 degrees. In 24-2, the outer most ring is not tested. Only those test points are included from 30-2; which are

known to be affected by glaucoma hence reducing the test time and yet achieving the same information as shown in figure 2.14.

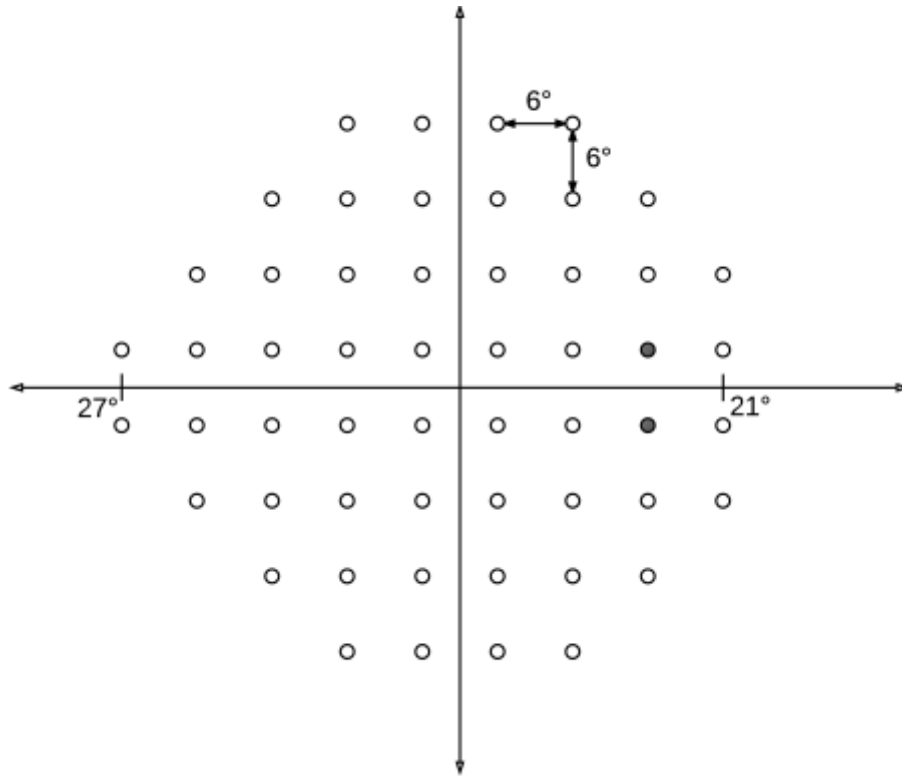


Figure 2.14: Testing 54 locations[14]

The central 10 degrees test gives higher resolution and better follow up of the central and macular vision . The difference between two test locations is 2 degrees as shown in figure 2.15.

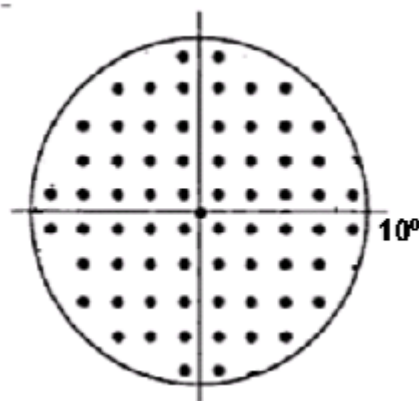


Figure 2.15: Measuring central field only[15]

It is important to monitor the patient who has advanced glaucoma and has signifi-

cantly lost his peripheral and central vision and the ophthalmologist wants to get more information about central region.

2.9 Humphrey Visual Field Tests

Two most commonly used tests for SAP are Humphrey and Octopus. Our thesis deals with Humphrey Visual Field tests.

2.9.1 Humphrey Visual Field Analyzer

HVFTs are performed using Humphrey Visual Field Analyzer (HVFA). The following figure shows the setup of HVFA. The patient has to rest his head on a chin rest while facing a white bowl of 30 cm radius enveloping his visual field. While measuring the monocular visual field of one eye; the other eye of the patient is covered. The analyzer presents a stimulus, and if that stimulus is seen by the patient; he triggers a button otherwise he shows no response.

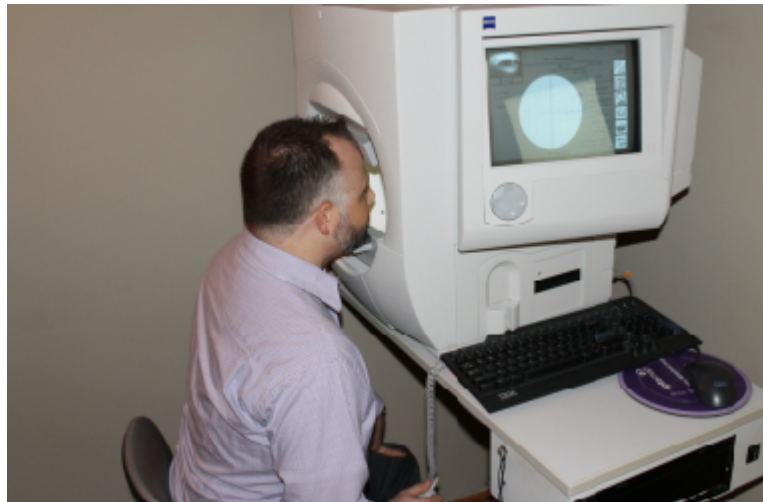


Figure 2.16: Humphrey Visual Field Analyzer[14]

The Humphrey perimeter as shown in figure 2.16 works in photopic conditions and uses background light of 31.5 abs and tests cones rather than rods using uses an attenuation scale of 0 to 50 dB (0 being the brightest). Since HVFA provides background illumination mainly hence it controls the contrast ratio of their stimuli.

The size of the stimulus follows Goldman standard for visual field tests in which the

diameter of the stimulus is presented in degrees. The size of each stimulus is four times the area of the one before it and ranges from 0.25 millimeter square to 256 millimeter square. The standard time of presentation of stimulus in HVFA is 200 ms or 0.20 seconds. HVFA is capable of varying the stimulus size from I to VI as shown in figure 2.17 and the default standard size is Goldman size III measuring 4 millimeter square.



Figure 2.17: Goldman sizes for stimuli [16]

2.9.2 Interpreting Humphrey Visual Field Reports

The above figure as shown in figure 2.18 shows the basic layout of an HVF test report. Every part has a significant meaning. First the top left portion contains the patient's data. The most important information which should be accurate is the age of the patient since the analyzer matches the sensitivity of stimulus points presented to the patient's eye with that of the healthy eye of the same age group. Hence wrong age will yield wrong results

Fig. 2.18 section 1 contains the reliability indices which tell the accuracy of the performed test. It contains the fixation loss, false positive and false negative errors. Fixation loss represents the number of times a patient responds to the target placed in his physical blind spot. The shutter of HVFA generates a sound before presenting a target; hence false positive errors represent the number of times a patient responds to the sound of the shutter. False negative errors represent the number of times a patient fails to respond to a target placed in his visual field and already seen by him because he may have lost his attention or maybe tired. These value of all these losses should be less than 33 percent [10] for the test to be reliable

Fig. 2.18 sections 2 and 3 give the grayscale or half tone plot and numeric display. The grayscale does not give very clear information and is not much useful. The numeric plot is the record in decibels of the sensitivity of patient's eye at the test locations where each value denotes the extent to which light can be dimmed and is still detectable by

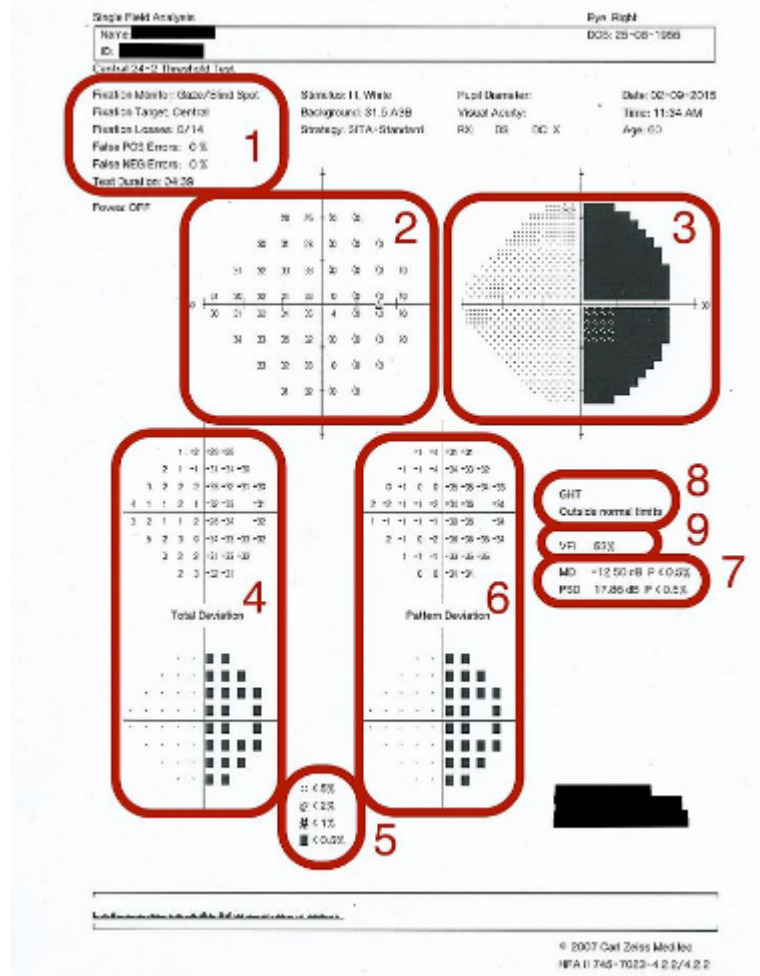


Figure 2.18: Humphrey Visual Field Test Report Pattern[14]

the patient. Fig.2.18 section 4 contains the numeric and graphic probability plots of total deviation. Total deviation gives us the difference between actual (sensitivity of patient) and expected sensitivity of the patient of same age (normal values recorded in the program). Fig.2.18 Section 6 gives the numeric and graphic probability plots of pattern deviation. The pattern deviation (PD) is derived from total deviation and is the most important data [10] since it eliminates any morbidity due to age of the patient or any other disease other than Glaucoma. PD is calculated by adjusting the measured thresholds upward or downward hence mitigating any generalized change in the threshold of the portion which is least damaged.

Fig.2.18 section 5 indicates the probability key symbols (PKS) which are relevant to the scope of this thesis. They are significantly depressed points and the presence of any of these in the PD indicates the onset of glaucoma. There are five types of probability key

symbols: $P < 0.5$ percent, $P < 1$ percent, $P < 2$ percent, $P < 5$ percent and the single dots (which represent normal functioning of the eye at that test location). $P < 0.5$ percent means that this is a normal value in less than 0.5 percent of the population and an abnormal value for the remaining 99.5 percent of the population. Fig. 4 sections 7, 8 and 9 contain values for mean deviation (MD), pattern standard deviation (PSD), Glaucoma hemifield test (GHT) and visual field indicator (VFI).

Mean Deviation gives us information about the hill of the vision. Greater the MD lower the height of the peak. MD of 6 indicates mild generalized depression. An MD value between 6 and 12 indicates moderate generalized depression and MD value greater than 12 indicates severe generalized depression.

PSD gives us information about the shape of the hill of the patient. Small PSD means homogeneous depression and large PSD indicates irregular depression of the hill of field of vision. PSD value of 1 indicates that all points are depressed homogeneously. Even if one point is more depressed; the PSD value will be higher. PSD should be less than 4 normally.

The values of MD and PSD combined give following information about visual field as shown in table 2.3.

Table 2.3: Information about Visual Fields from MD and PSD[16]

| MD | PSD | The Visual Field |
|----------|----------|---|
| Normal | Normal | Normal or very minimally disturbed |
| Abnormal | Normal | Pure generalized depression (whole field depressed homogeneously) |
| Normal | Abnormal | A small purely localized defect or an artifact is present |
| Abnormal | Abnormal | A large defect present with a significant localized component |

GHT helps to compare the sensitivities of the upper and lower hemisphere of an eye. Normally the sensitivity of upper and lower half should be identical but glaucoma can causes sensitivities of the hemispheres to change. GHT is specifically designed for glaucoma and the upper and lower hemispheres are divided into identical zones and the sensitivity of the zones is compared with each other. Sometimes a lesion may also result in sensitivities to change. GHT test produces one of the following outputs:

CHAPTER 2: VISUAL FIELD TESTS

- Outside normal limits
- Borderline
- Generalized reduction in sensitivity
- Abnormally high sensitivity
- Within normal limits

The VFI value of less than or equal to 78 percent indicates early glaucoma; the value between 78 and 91 indicates moderate glaucoma and greater than 91 indicates severe glaucoma.

CHAPTER 3

LITERATURE REVIEW

3.1 Glaucoma : The Optic Neuropathy

A study done in May 12, 2010 by Carlos Gustavo V. De Moraes et. al [17] investigated the IOP dependent and IOP independent factors which may lead to glaucoma progression in a treated glaucoma. The study was done on 587 eyes of 587 patients having mean age 64.9 years including 58 percent women patients from which 90 percent were of European descent. The common diagnosis in patients was open angle glaucoma. The study revealed old age, exfoliation syndrome, decreased central corneal thickness, detected disc hemorrhage, para-papillary atrophy and IOP peak as increased risk factors of glaucoma progression in the patients who have a treated glaucoma.

Another study done by Carlos Gustavo V. De Moraes et al [18] in July 2017 investigated whether glaucoma affecting both the hemifields progresses rapidly then that in which the single hemifield is affected. The study was conducted on 205 eyes of 205 patients having mean age of 64.2 years and mean follow up time of 6.5 years. The patients were divided into three groups; the first having initial superior defect known as group A, the second group B having initial inferior defect and group C having both hemifields involved. The results showed that the glaucoma in patients in group C progressed faster than those in groups A and B hence indicating more aggressive therapy for the eyes of the patients which have both hemifields affected.

A famous study conducted in September 14, 2009 known as ADAGES (The African Descent and Glaucoma Evaluation Study) done by Pamela A. Sample et. al [19] identified the factors differing in the onset and rate of progression of glaucoma between the patients

of African and European ancestry. ADAGES was initiated and funded by ational Eye Institute because several studies showed that people with African descent have a high probability of developing open angle glaucoma as compared to people with European descent [20] [21] [22].This prospective, multicenter observational cohort study included 1221 participants of African and European descent having no glaucoma (normal), suspected glaucoma, and glaucoma. The factors which were measured in all the patients were baseline demographics ,optic nerve structure,visual function risk factors and the clinical status.The people with African descent showed a high percentage of diabetes; high blood pressure, thin corneas and low percentage of heart disease as compared to the people with European descent. There were no differences in the IOP found in the two groups.

ADAGES was futher extended to ADAGES II in May 2010 by the research done by Christopher A. Girkin et. al. [23] defined the differences in optic disc, retinal nerve fiber layer, and macular structure between healthy participants of African and European descent using the quantitative imaging techniques in the ADAGES study described above. 648 healthy subjects participated in ADAGES and images were obtained using stereoscopic photography, confocal scanning laser ophthalmoscopy (Heidelberg retina tomography [HRT]), and optical coherence tomography (OCT) . The gender, hypertension and the diabetes were compared for the two groups of people including 634 eyes of 326 african and 630 eyes of 322 european people.This study showed significant differences in the optic nerve variables for participants with AFfrican and European descent.

3.2 Standard Automated Perimetry

Artes et al. 2002 [24] made a comaprison between Full Threshold, SITA Standard and SITA Fast. Figure 3.1 shows that SITA Fast is the fastest amongst the three; reducing testing time to approximately 5 minutes for an eye. However studies have shown that SITA Fast has has less sensitivity in determining Visual Field Defects as compared to SITA Standard ; hence uptil now SITA Standard remains the most widely used detection algorithm [25].

A retrospective study conducted in June 20,2014 by Ryo Asaoka included [26] 128 eyes of 128 patients. It used ‘Hierarchical Ordered Partitioning And Collapsing Hybrid –

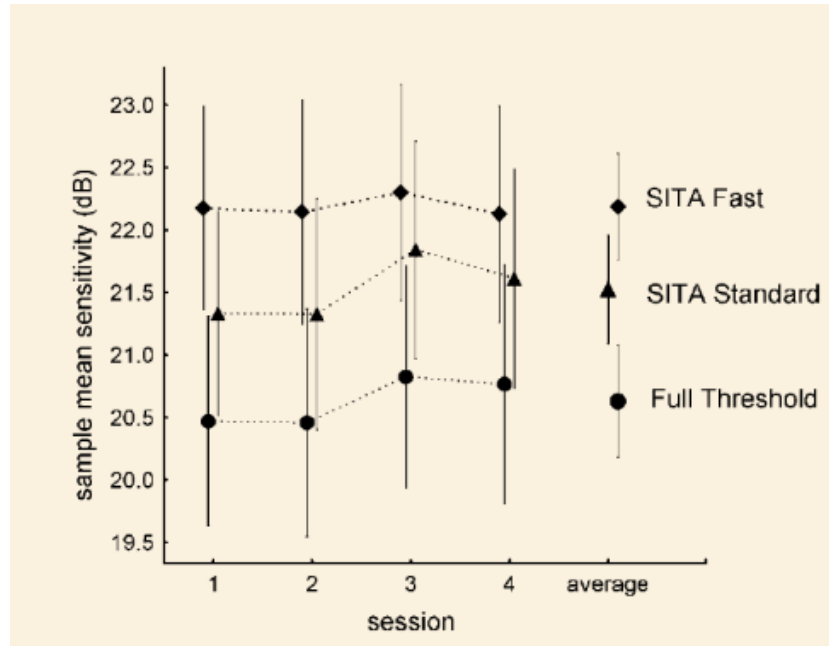


Figure 3.1: Comparison between Full Threshold, SITA Standard and SITA Fast [24]

Partitioning Around Medoids' algorithm to cluster values from 30-2 and 10-2 visual fields in order to map the damaged regions due to glaucoma. 142 total deviation values including 74 values from the 30-2 visual field reports and 68 values from the 10-2 visual field reports were used as the database. The stable clusters were then evaluated using bootstrapping. The tests were done using SITA Standard and using a stimulus size of Goldmann III. Research Ethics Committee of the Graduate School of Medicine and Faculty of Medicine at the University of Tokyo approved the study and the data was collected from the hospital and used for research using written consent of the patients. The study showed the presence a large number of sectors 10-2 visual field which were absent in the 30-2 visual fields hence suggesting that ophthalmologists should use 10-2 tests along with 30-2 visual fields to examine the damage in the central ten degrees for advanced glaucomatous patients. The results of this study is shown in figure 3.2.

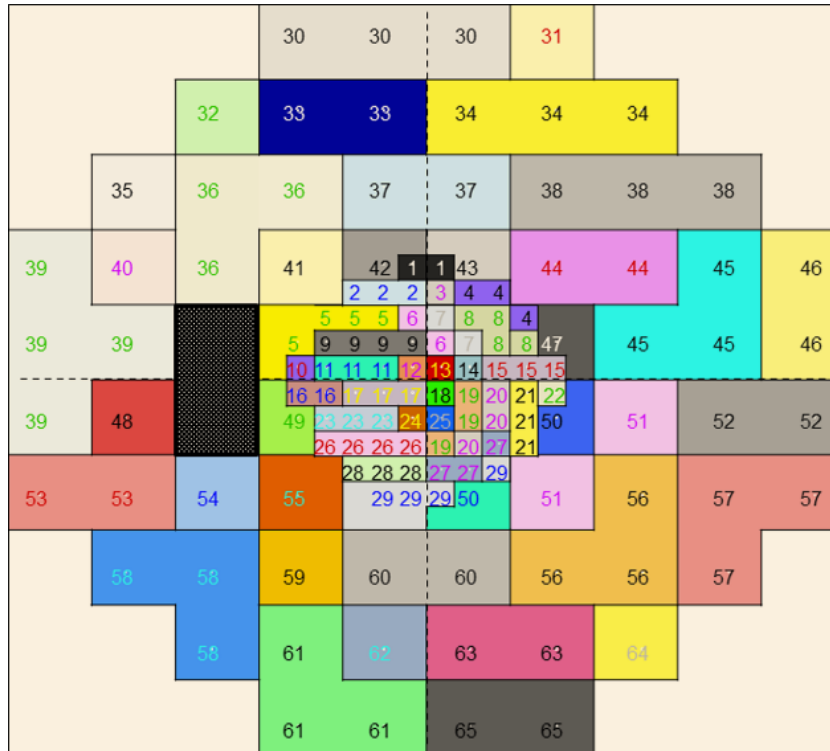


Figure 3.2: Total 65 sectors were obtained: 38 sectors from 30-2 and 29 sectors from 10-2 visual fields[26]

An observational study done in May 2012 by Sung Chul Park et al. [27] compared 10-2 versus 24-2 visual fields for detection of progression of initial parafoveal scotoma (IPFS) in glaucomatous eyes. 50 patients were included having mean age of 62 years and mean follow-up period of 5.7. The results showed more significant progression of IPFS in 10-2 test as compared 24-2 analyses especially in the central 10 degrees region.

A recent cross sectional cohort study done in July 2017, by Dana M. Blumberg et al.[28] determined the association between quality of life (QOL) and reports off 24-2 and 10-2 visual fields in patients with primary open-angle glaucoma. The data of 113 glaucomatous patients using standardized binocular 24-2 and 10-2 visual field tests was collected from a tertiary care specialty practice from May 2014 to January 2015 and the was analyzed from from March 2016 to May 2016. The results revealed a very significant clinical implication that although the majority of the ophthalmologists traditionally think of performing 10-2 visual fields only in advanced disease, when a patient’s island of vision has grown so constricted that the 24-2 visual field no longer provides much useful information. However, this study showed the macular damage may occur early in the

glaucoma as well in the central 8 or 10 degrees and hence the QOL of life of glaucomatous patients is more associated with 10-2 rather than 24-2. Hence ophthalmologists should pay attention in performing 10-2 test even in the start of glaucoma. The results of this study are shown in figure 3.3.

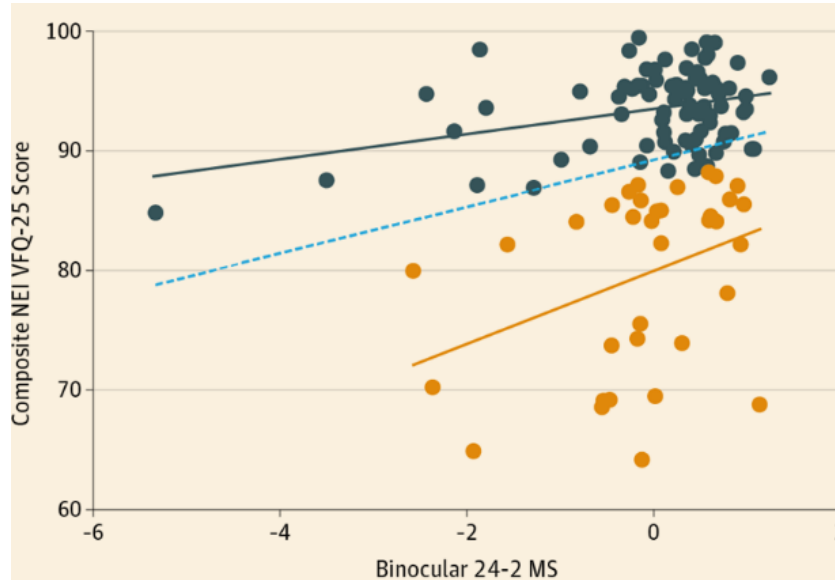


Figure 3.3: 10-2 visual field is affected in early glaucoma as well [28]

A study done by Carlos Gustavo V. De Moraes et. al. in July 2012 [29] studied the reasons of disparities among three main prime diagnostic techniques of glaucoma: standard automated achromatic perimetry (SAP), optical coherence tomography (OCT) and multi focal visual evoked potential technique (mfVEP). It was a prospective cross-sectional study containing 138 eyes of 69 patients having glaucoma which were tested using SAP OCT and mfVEP. If the results of 2 out of these three techniques were same showing a lesion at the same location then that lesion was considered a true glaucoma defect. But if this defect was missed by the third test then the reasons for this disparity were analyzed. The study revealed that the results of all these three techniques were mostly consistent. However the fewer cases showing inconsistency in the results of these three methods is due to modalities and limitations of the test itself and the ophthalmologist should better understand the limitations of each test and should consider which test is best to perform in which situation.

A study done by Yaniv Barkana et. al [30] in June 2006 analyzed whether the mean deviation (MD) or the reliability of the SITA-Standard 24-2 test is affected by the order

of eye testing or not. 47 patients including 18 men and 29 women were enrolled in the study. Two consecutive 24-2 Standard SITA sets were done for every patient for the right eye. These patients showed glaucoma hence they were enrolled in the study. Afterwards; a followup test was performed on the left eye first and then on the right eye. The results of patients are affected by fatigue; hence ophthalmologists suggest checking the affected eye first. The 30-2 test requires approximately 15 minutes per eye (including the rest breaks taken by the patient) whereas 24-2 requires approximately takes 7 minutes per eye [8]. This cohort study showed the mean deviation or the reliability of the SITA Standard 24-2 test is not affected by the order of the eyes and fixation loss affects the test results and is also not affected by the order of the eyes being tested.

3.3 Scoring Glaucoma

In August 2004 [31], a clinical research by J.D. Henderer et. al. emphasized on using glaucoma staging to analyze, detect and treat glaucoma. The research stated the fact that optic nerve analysis provides ample information regarding patient's disease, however the severity of disease is not reflected solely from optic nerve analysis. The article focused on VFT interpretation which helps ophthalmologists to identify the damage occurred due to glaucoma progression. Two common glaucoma staging systems Hodapp Parrish Anderson (HPA) and Spaeth Field Damage Likelihood Score (FDLS) were explained and analyzed by the author as shown in table 3.1 and table 3.2.

In a research study by Remo Susanna Jr. and Roberto M. Vessani[32], significance of glaucoma staging i.e. mild, moderate and advanced was stated to improve the disease management. The research stated standard automated perimetry / visual field test is an effective method to quantify glaucoma damage. Among the standard staging systems being used to classify stages of glaucoma from standard automated perimetry tests, Hodapp, HPA staging system is a popular one. HPA classifies VFTs into four stages. Another glaucoma score system i.e. Advanced Glaucoma Intervention Study (AGIS) is being used to stage glaucoma. This system classified VFT into five stages i.e. early, moderate, advanced, severe and end stage. Collaborative Initial Glaucoma Treatment Study (CIGTS) visual field score is another scoring standard being used for glaucoma staging. However, lack of accuracy in results exists in VFTs due to false positives/ false negatives. Such inaccuracies were addressed by a new Visual Field Staging System by

the University of São Paulo Glaucoma Visual Field Staging System (USP-GVFSS). The proposed system included a new parameter visual field index (VFI). Along with the degree of damage, it included the location of damage. Thus improved glaucoma staging and analysis.

A clinical study was conducted by Rasker, Marga TE, et al. on [33] effect of glaucoma progression in visual field tests. Dataset comprised of Visual field tests for 9 years annually with automated perimetry. Dataset comprised as shown in table 3.3.

Rate of loss in visual field tests was observed 3 percent per year for all the three categories. Moreover, the rate of decline in visual field is not related to either the initial visual field status or presence of disc hemorrhages. A linear relationship was observed only in the patients with progression in visual field.

Chakravarti, Tutul [34] in a clinical research analyze the accuracy and limitations of HPA staging algorithm for staging and detection of early glaucomatous damage. The review was conducted on VFTs of 183 Ocular Hypertensive (OH) subjects. The frequency of subject analysis was twice in every seven years. Visual field analysis tests identified 22 patients (27 fields) out of 183 with early glaucoma.

A comparison study by M. Ng et. al. [35] in October 2013 on visual field test severity classification system between three standard scoring systems Advanced Glaucoma Intervention Study scoring system (AGIS), Glaucoma Severity Staging system (GSS), and Enhanced Glaucoma Severity Staging system (eGSS) was done. Glaucoma classification was done using MD, PSD and VFI. Figure 3.4 shows Tthat MD and PSD distributions appear broader in AGIS and GSS than in eGSS; this is likely due to the fact that eGSS relies on these two global indices in staging severity [36].

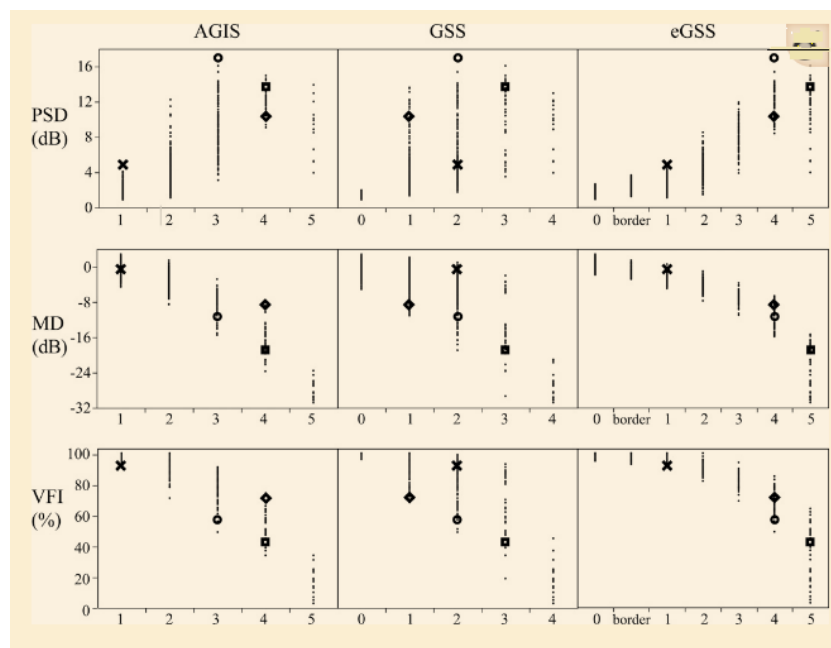


Figure 3.4: PSD,MD and VFI according to staging systems AGIS, GSS [36]

Table 3.1: Hodapp Parrish Anderson Staging System[31]

| Stage | Definition |
|----------|--|
| Minimal | <ol style="list-style-type: none"> 1. Abnormal glaucoma hemifield test 2. Corrected pattern standard deviation depressed at the P<5percent level (or pattern standard deviation of P<5percent on a SITA field) 3. A cluster of three non-edge points (for a 30-2 field) in an expected location for glaucoma, all of which are depressed on the pattern deviation plot at the 5percent level (or greater) and at least one of which is depressed at the 1percent level (or greater) |
| Early | <ol style="list-style-type: none"> 1. Mean deviation <-6 dB 2. No point at 5° from fixation is less than 15 dB. 3. The total number of points depressed at the 5percent level or worse on the pattern deviation plot is less than one quadrant, while the number of points depressed at the 1percent level or worse is less than one-half of a quadrant or one-eighth of the field |
| Moderate | <ol style="list-style-type: none"> 1. Mean deviation between -6 and -12 dB 2. One point at 5° from fixation measures <15 dB 3. The total number of points depressed at the 5percent level or worse on the pattern deviation plot is less than two quadrants, while the number of points depressed at the 1percent level or worse is less than one quadrant |
| Severe | <ol style="list-style-type: none"> 1. Mean deviation >-12 dB 2. One point at 5° from fixation of 0 dB 3. One point in each hemifield at 5° from fixation measures <15 dB 4. The total number of points depressed at the 5 percent level or worse on the pattern deviation plot is greater than two quadrants, while the number of points depressed at the 1 percent level or worse is greater than one quadrant |

Table 3.2: The Field Damage Likelihood Score [32]

| Stage | Grading by Visual Field Area | Grading by Number of Abnormal Points |
|---------------------------|--|--------------------------------------|
| 0 (no loss) | None | 0 |
| 1 (minimal loss) | Early nasal step | 1 to 3 |
| 2 (mild loss) | Less than one-half of one quadrant lost | 4 to 6 |
| 3 (mild-to-moderate loss) | Approximately one quadrant lost | 7 to 12 |
| 4 (moderate loss) | Approximately one to two full quadrants lost | 13 to 22 |
| 5 (marked loss) | Approximately two to three full quadrants lost | 23 to 32 |
| 6 (advanced loss) | More than three quadrants lost | 33 to 42 |
| 7 (far advanced loss) | Residual island <25 degrees or central island <4 degrees | 43 or higher |

Table 3.3: DATASET BY RASKER, MARGA TE, ET AL [33]

| Category | Count |
|------------------------------------|-------|
| Normal Pressure Glaucoma (NPG) | 34 |
| Primary Open Angle Glaucoma (POAG) | 68 |
| Ocular Hypertension Glaucoma (OHG) | 125 |

METHODOLOGY

The chapter first presents the method for extraction of region of interest from rest of the image followed by removal of undesired objects. Then the algorithm for extracting significantly depressed PKS elements is presented. Further; their count and location in each quadrant is extracted and finally the algorithm for grading glaucoma pattern is presented. The block diagram of the proposed methodology is shown in figure 4.1

4.1 Extraction of Region of Interest

The entire image of one HVFT report at one time is imported into MATLAB's working directory as shown in figure 4.2.

In order to detect glaucoma and categorize it depending upon the severity (mild, severe) of disease from VFTs, Region of interest (ROI) should be extracted from the scanned VFT report. ROI is extracted to get the time optimum results i.e. rather on applying image processing on full scanned VFT image, processing is done on ROI. In VFT, Pattern deviation map is the ROI for glaucoma detection as it is the most significant data and contains visual field defects only due to glaucoma. Input image is converted into binary image using Otsu's segmentation proceeded by formation of two vectors VRSUM, VCSUM with dimensions $[1 \times R]$, $[1 \times C]$ containing sum of entries of all rows and sum of entries of all columns respectively. In each VFT, Pattern deviation (PD) map is the last map thus its location varies slightly in each of the VFT. Moreover, width 'W' and height 'H' of PD map remains same in each VFT report. Considering this property of PD map minimum value from the range of rows and columns with probability of

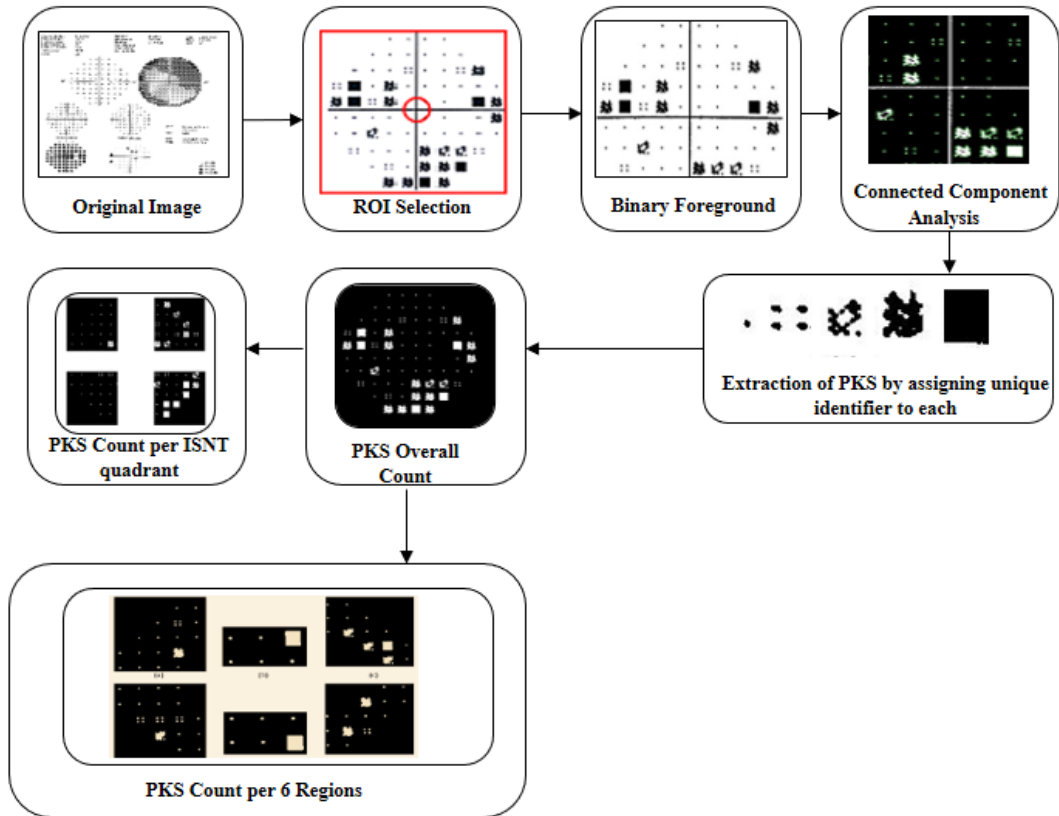


Figure 4.1: Block Diagram of Proposed Methodology

containing PD map is extracted from VRSUM, VCSUM i.e. MinR and MinC. Figure 4.2 with green and red highlighted portions indicates the region having probability of PD map. Asterisk ‘*’ indicates the minimum value in the highlighted region. I (MinR, MinC) is the center position of PD map. Taking I (MinR, MinC) as center point a region of width ‘W’ and height ‘H’ is extracted which results in the desired ROI i.e. PD map as shown in the figure 4.3

4.1.1 Extraction of Green Channel

The colored ROI in figure 4.3 contains three channels : red, green and blue. The green channel is closest to human perception and contains the most of the information. We extracted green channel for the ROI which got rid of the unwanted background since the background belonged to the red channel. The extracted foreground in the green channel is shown in figure 4.4.

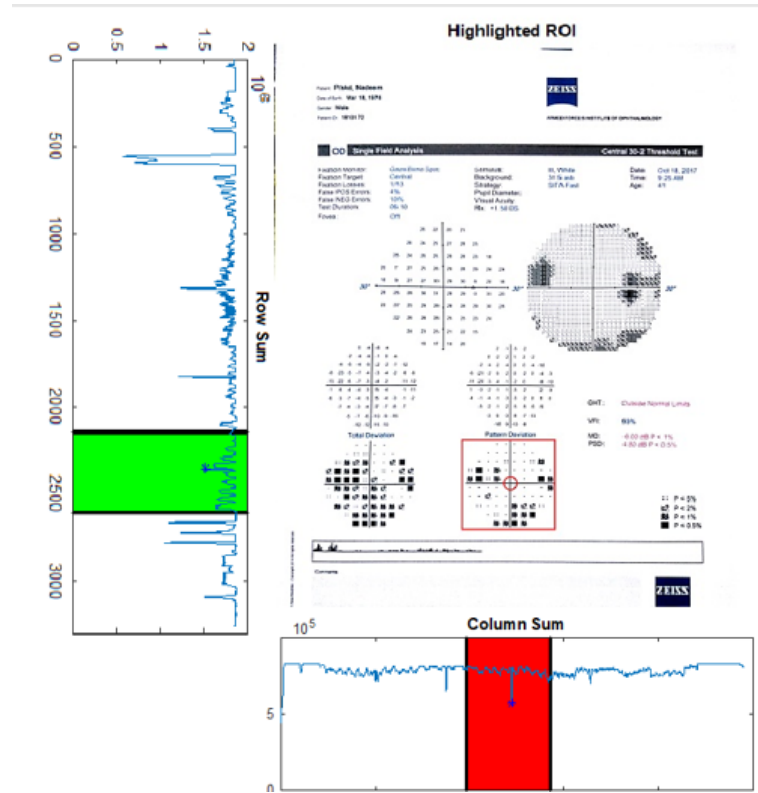


Figure 4.2: Original HVFT Report Imported into MATLAB with the ROI highlighted

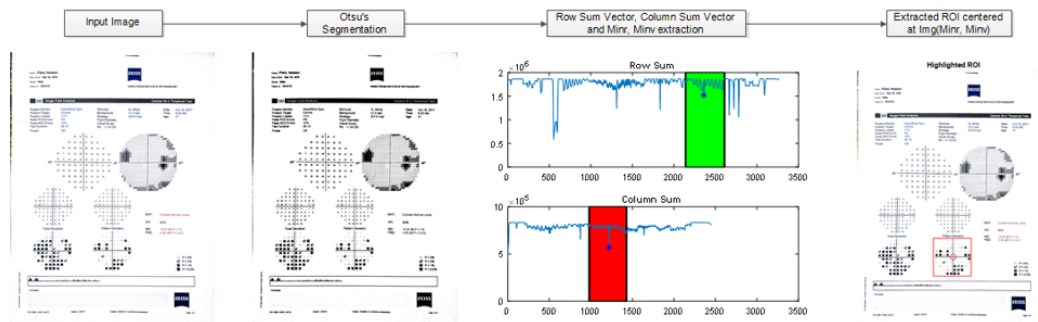


Figure 4.3: ROI Extraction from the entire HVFT Report (a): Input Image (b): Otsu's segmentation (c): Row sum vector and column sum vector and minR, minV extraction (d): Extracted ROI centered at $img(\min R, \min V)$

4.1.2 Binarizing the Cropped Image

In image processing we convert the images to binary to find our region of interest. The pixels that we are interested to work with further are given a value of 1 and others are made zero. When we convert to binary, the foreground is given value 0 and the

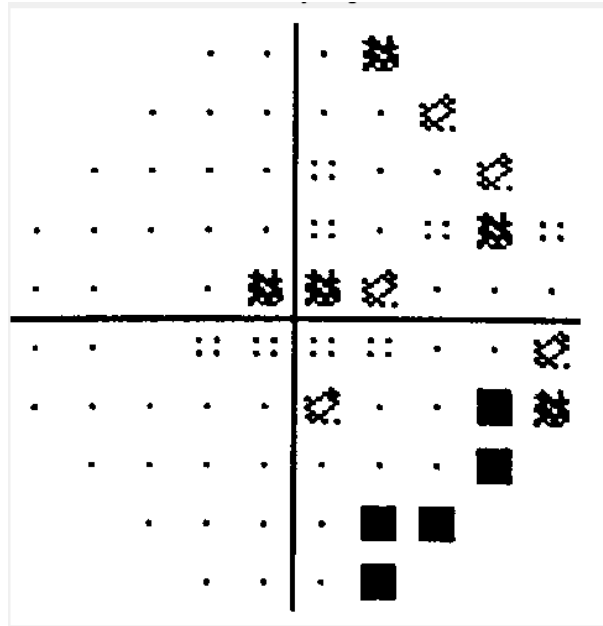


Figure 4.4: Extracted Green Channel

background is given the value 1. We invert this assignment so that the background is in black and foreground is in white. This is done so that we may perform any operation we want with the individual blobs or objects of foreground like connected component analysis, filtering, thresholding etc. Figure 4.5 shows the inverted binary image for our region of interest.

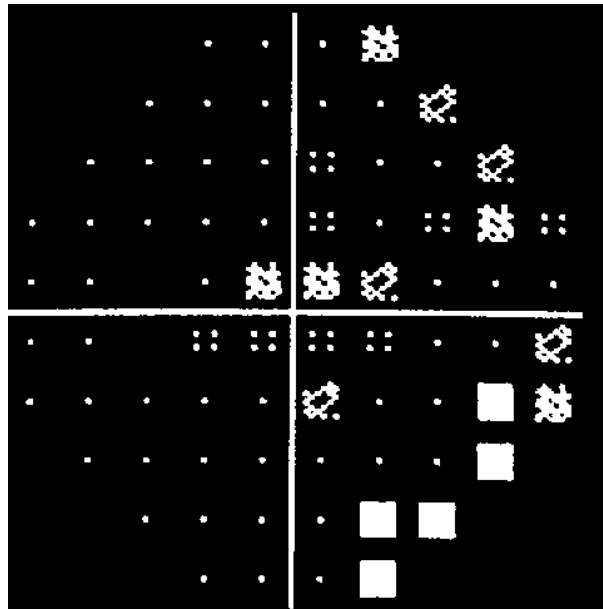


Figure 4.5: Inverted Binary Image

4.1.3 Connected Component Analysis

In order to do further processing; we perform connected component analysis (CCA) of the binary image in figure 4.5. CCA also known as blob extraction or region labeling is done to find the 4 (pixels connected by faces) or 8 connectivity (pixels connected by faces and edges) of components in an image and is an application of graph theory[37]. The resulting blobs are then labeled according to the specified heuristics. Connected component labeling can operate on a variety of information [40]. Figure 4.6 shows the illustration of 4 and 8 connectivity of connected neighbors.

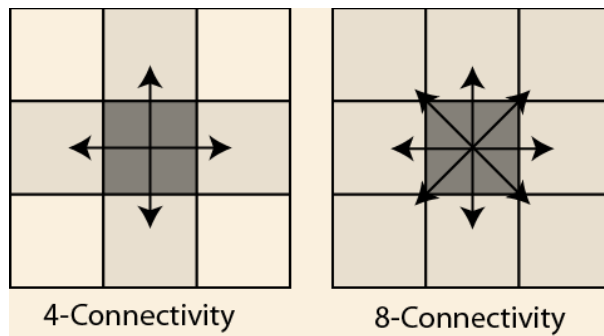


Figure 4.6: Connected components in image processing having pixels connected by their faces (4-connectivity), or by their faces and edges (8-connectivity) [38]

Each connected component is then assigned a unique label.

4.1.4 Removal of Axes

Figure 4.5 contains the major and minor axes. These axes are undesirable objects in our case. In order to get rid of them, we calculated the area of all of the objects obtained through CCA and filtered the largest objects; since these axes occupy the largest area. Keeping the objects in the range [1:1000] eliminates the unwanted axes.

4.2 PKS extraction

The probability key symbols (PKS) which are focus of this thesis are extracted after the removal of the axes as shown in figure 4.7.

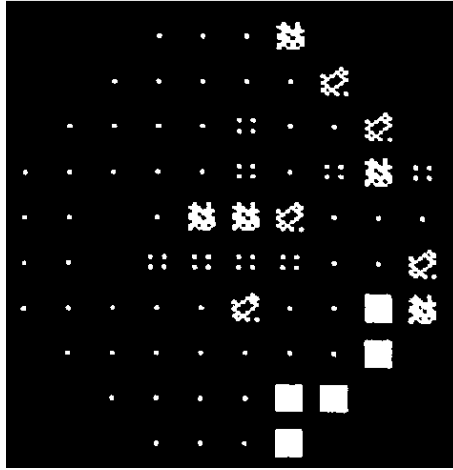


Figure 4.7: Figure containing only the key elements extracted

4.3 PKS labeling

Referring to section 2.9.2 and figure 4.7 it can be seen that there are five types of PKS enlisted as follows:

- Single dots representing normal healthy functioning of eye:



- Probability less than 5 percent points:



- Probability less than 2 percent points:



- Probability less than 1 percent points:



- Probability less than 0.5 percent points:



The probability values of these symbols is significant as lower the value higher the significance. The probability less than 0.5 percent points indicate the creation of complete scotoma (blind spot) due to glaucoma in the patient's visual field. We use the statistical properties to segregate these PKSs. The 7 properties that we used along their descriptions are listed as follows:

- **Area:** Number of pixels in a region returned as a scalar quantity.
- **Major Axis Length:** Length of the major axis of ellipse having the same normalized second central moments as those of the region.
- **Minor Axis Length:** Length of the minor axis of ellipse having the same normalized second central moments as those of the region.
- **Eccentricity:** Ratio of the distance between major axis length of ellipse and foci of the ellipse.
- **Perimeter:** Distance of the boundary around the region.
- **Solidity:** Proportion of the pixels in convex hull of the region.
- **Extent:** The ratio of pixels in the region to pixels in the bounding box.

As can be viewed in figure 4.7 the single parameter or region property that can be used to segregate all of these PKS is that of the area. Most apparently the single dots occupy the least area. We segregate these dots by filtering the objects covering the least area. However, when we apply this segregation, the probability less than 5 percent points which look like almost connected four dots also get segregated as shown in figure 4.9.

We solve the issue shown in figure 4.9 by using the isotropic dilation to cluster almost connected (disconnected components which are very near to each other) components.

As shown in figure 4.8 there are 87 distinct objects detected but we want the four dots to be detected as one clump (cluster). Hence we use isotropic dilation along with CCA to

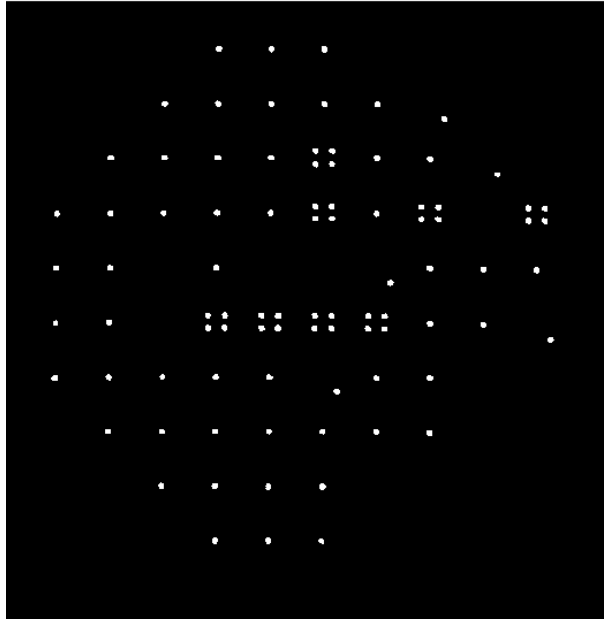


Figure 4.8: Single and Four dots combined

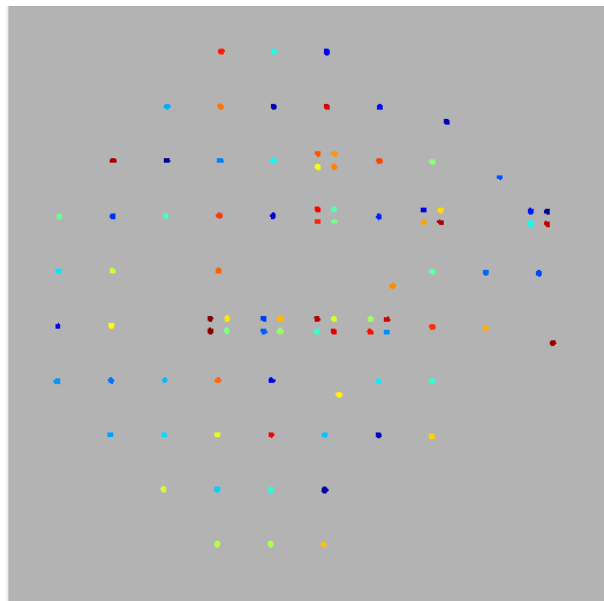


Figure 4.9: 87 distinct objects detected

achieve this purpose. Instead of dilating the objects, we use euclidean distance to compute distance transform and then threshold the result. This technique of thresholding the distance transform is called isotropic dilation. This is used because it is very fast as compared to conventional dilation in MATLAB. We assume that the four dots would be fully connected (one object) if they would be lets say 6 pixel units apart. Hence we threshold the euclidean distance transform at 6 pixel units and cluster the clumps of

four dots as shown in figure 4.10. The single four dots are also dilated but they remain a separate entity since there is no other object in their vicinity of 6 pixel units distance as shown in figure 4.10. The clustered clumps occupy large area as compared to the single dots hence we separate them by using area as the segregation parameter as shown in figure 4.11.

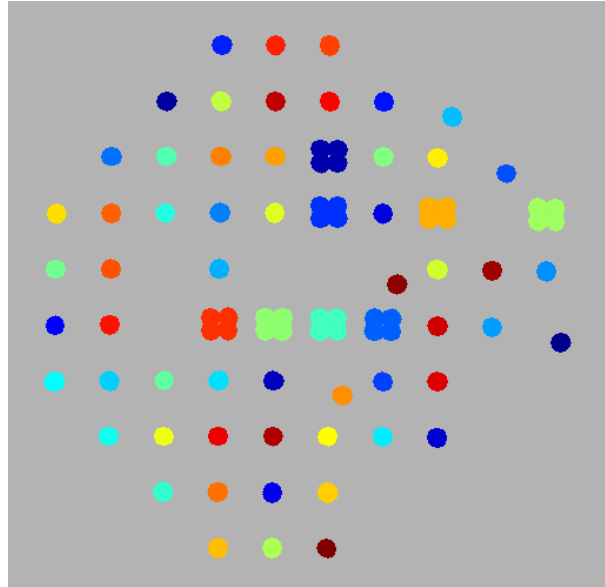


Figure 4.10: Clustered four dots using isotropic dilation

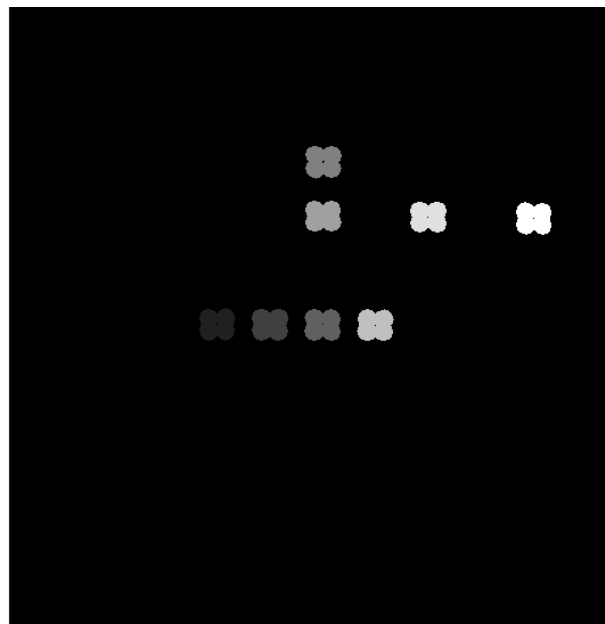


Figure 4.11: Probability less than 5 percent points segmented

After separating the probability less than 5 percent points, we for the time being ignore single dots and turn our attention to the remaining three types of blobs PKS which are the three largest blobs as well as shown in figure 4.12. As shown in figure 4.12 the probability less than 0.5 percent points occupy the largest area but area alone is not enough for classification. We use four features of eccentricity, solidity, extent and parameter to segregate squares from the rest of the PKS. The result of segregation is shown in figure 4.13.

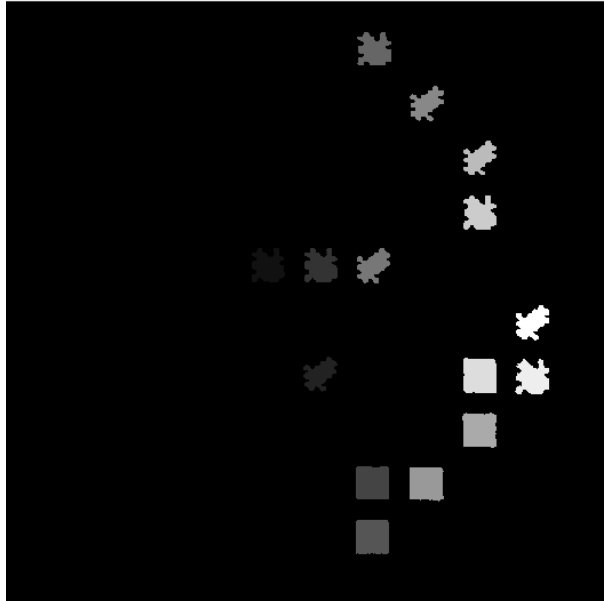


Figure 4.12: Three largest blob PKS

After the segregation of probability less than 0.5 percent points we are left with probability less than 2 and 1 percent points as shown in figure 4.14.

In order to segment $P < 1$ percent points we use and threshold the features of minor axis length, major axis length, eccentricity and parameter. The idea behind segregation is that we find all the indexes which follow this segregation rule e.g all the indexes having minor axis length, major axis length, eccentricity and perimeter in a certain characteristic range. By accessing the label matrix, we find all those indexes in the original image and give them a specific identifier; giving zero label to all the rest of the indexes which do not follow the defined rule. We then create a separate image of the keeper indexes and obtain the segregated desired objects. The probability less than 1 percent points are shown in figure 4.15.

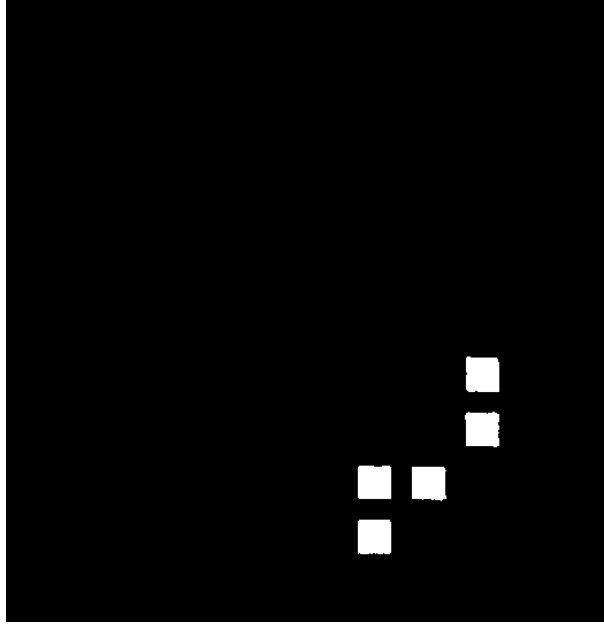


Figure 4.13: Probability less than 0.5 percent points segmented

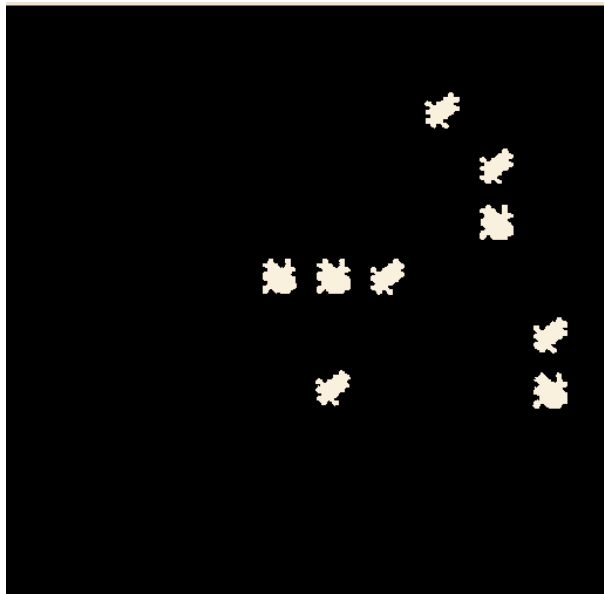


Figure 4.14: Probability less than 2 and 1 percent points

The problem in segregating the probability less than 2 percent points is that they have a disconnected dot as shown in figure 4.7. We need to separate this disconnected dot with the single dots that represent normal functioning of the eye. To get these disconnected dots appear at their proper location we use the process of image subtraction. We perform three subtractions yielding our results. First of all we subtract figure 4.11 from figure 4.7 resulting in the figure 4.16.

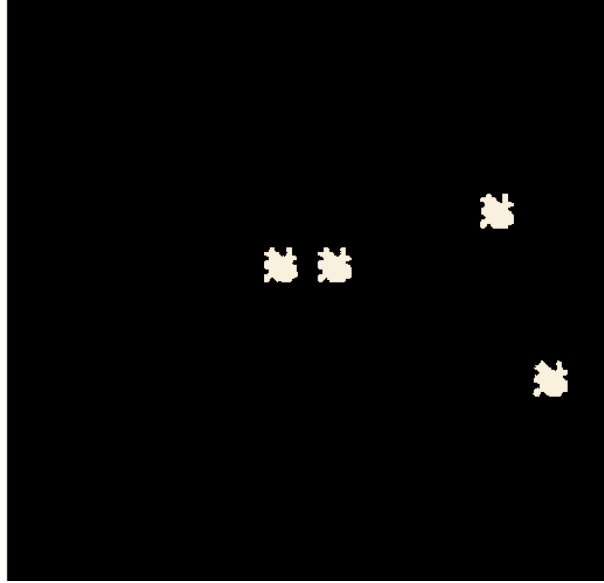


Figure 4.15: Probability less than 1 percent points segregated

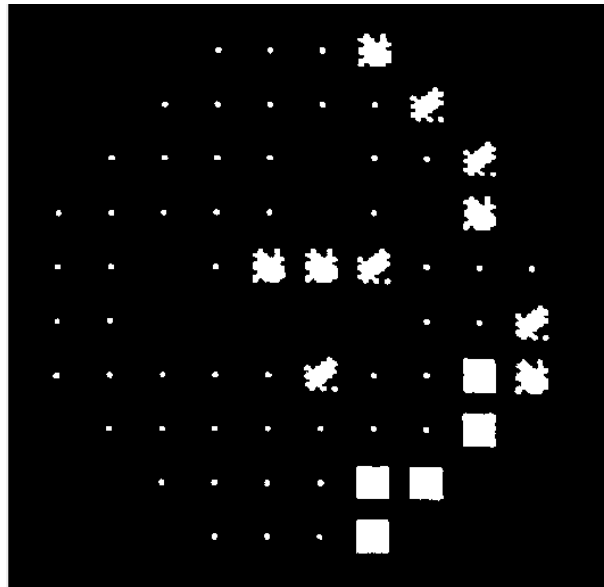


Figure 4.16: Result of first image subtraction

In first subtraction we have subtracted the image containing segregated probability less than 5 percent points from the original image containing PKSs. We are left with the image shown in figure 4.16. After this, we perform the second subtraction of figure 4.16 from figure 4.13 yielding in figure 4.17. In second subtraction we have subtracted the image containing segregated probability less than 0.5 percent points (figure 13) from resultant image after first subtraction (figure 16). We are left with the image shown in figure 4.17. After this, we perform the third and final subtraction of figure 4.17 from

figure 4.15 ; therefore subtracting $P < 1$ percent points from the PKS image. The results are shown in figure 4.18.

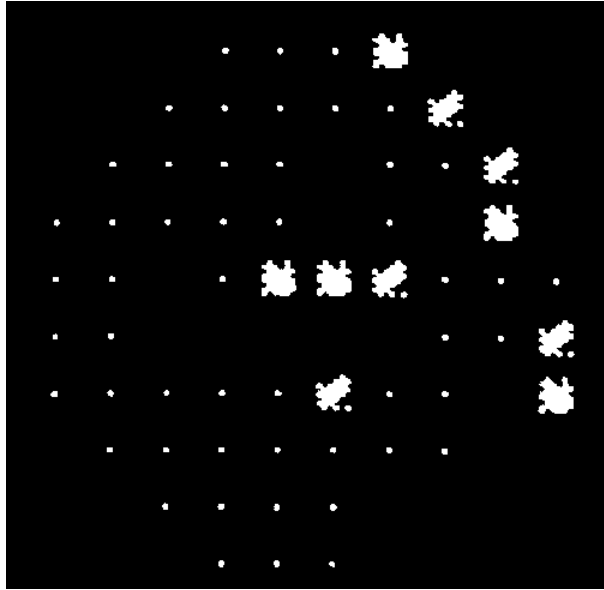


Figure 4.17: Result of second image subtraction

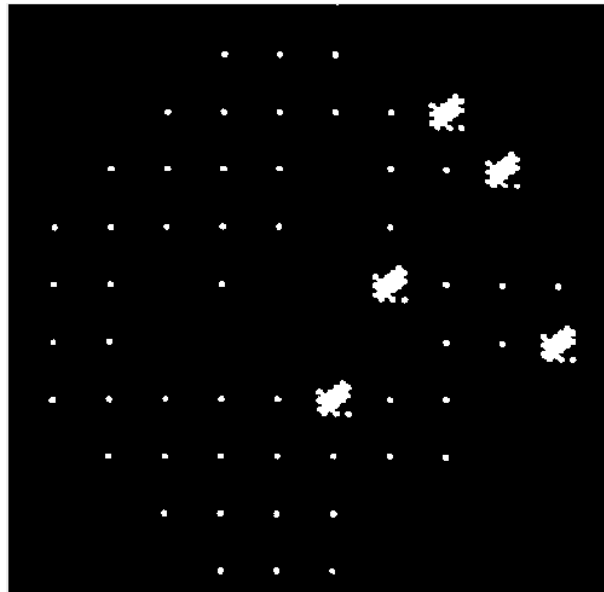


Figure 4.18: Result of third image subtraction

Hence after three subtractions we are left with single dots and probability less than 2 percent points as shown in figure 4.18. Again in order to separate single dots from probability less than 2 percent points we use the concept of isotropic dilation discussed in detail above. The threshold for distance used here is 4 pixel units. The resulting

image is shown in figure 4.20. We then use area to segment our final two PKSs as shown in figures 2.21 and 2.22.

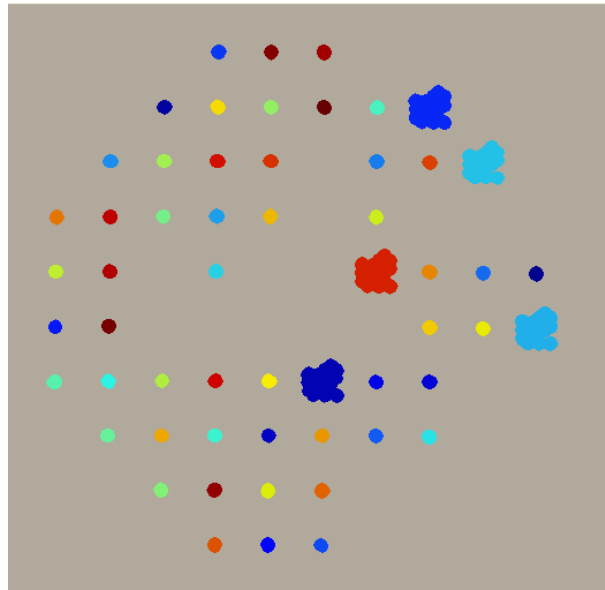


Figure 4.19: Clustered single dots and probability less than 2 percent points

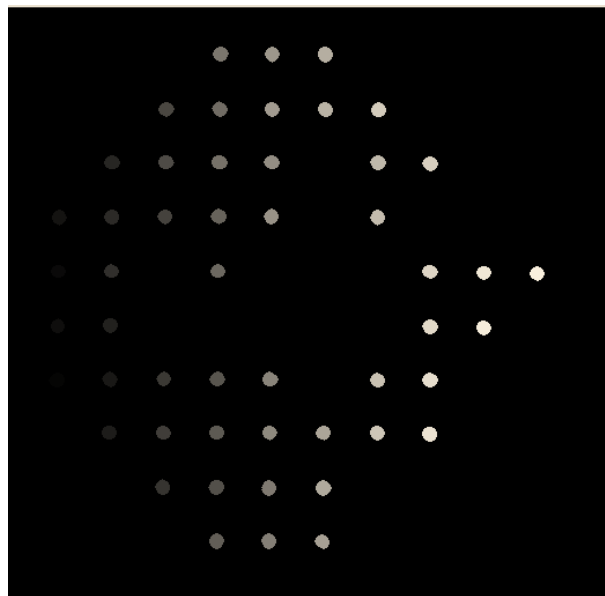


Figure 4.20: Single dots segregated



Figure 4.21: Probability less than 2 percent points segregated

4.4 Overall PKS count and Quantitative Score

After successful PKS extraction (discussed in section 4.2) and PKS labeling (discussed in section 4.3) we get the count of each individual PKS in the PD plot of HVFT report. As shown in figures 4.12, 4.14, 4.16, 4.21 and 4.22 the counts of each individual type of PKS is tabulated in Table 4.1

Table 4.1: Overall count of each PKS segregated and classified

| PKS | Reference Figure | Count |
|-------------------------|------------------|-------|
| Single dots | 4.21 | 51 |
| P less than 5 percent | 4.12 | 8 |
| P less than 2 percent | 4.12 | 5 |
| P less than 1 percent | 4.16 | 4 |
| P less than 0.5 percent | 4.14 | 5 |

The results of the table 4.1 are in consistency with the figure 4.7. We need to score these PKSs such that these scores are significant and correct clinically. Much work has been done on scoring of decibel values in the total deviation plot as discussed in Chapter 3. However, very less work has been done on assigning quantitative scoring to the PKS symbols depicted on the PD plot. We use the quantitative scoring used by SCHEIE (Systematic classification of Humphrey Visual Fields-Easy Interpretation and Evaluation) method [41] to grade the PKS symbols detected in section 4.3. The following figure 4.22 explains the definition of significant points according to the SCHEIE scoring criterion.

| Value | Rule |
|--------|---|
| <0.5 % | One point counts |
| <1 % | One point counts |
| <2 % | A point only counts if it is next to a <2%, <1%, or <0.5% point in the same hemifield. The points may be in contact diagonally. |
| <5 % | This point never counts for itself and never causes a <2% point to count. |

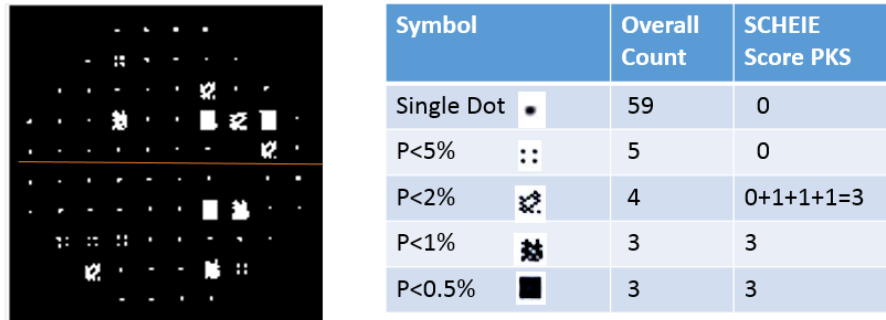
Figure 4.22: SCHEIE Rules for scoring Glaucoma

According to SCHEIE criterion, a point with <5 percent probability is not considered significant. A point with <2 percent probability is only considered significant if adjacent to a <2 percent, <1 percent or <0.5 percent point in any horizontal, vertical, or diagonal direction. Points with <1 percent and <0.5 percent probability are considered significant by themselves. Following this rule of scoring PKSs the score of our extracted PKS is shown in Table 4.2.

Table 4.2: Count and scoring of PKS in the overall image according to SCHEIE criterion

| PKS | Reference Figure | Count | Quantitative SCHEIE Score |
|-------------------------|------------------|---------------|-----------------------------------|
| Single dots | 4.21 | 51 | None |
| P less than 5 percent | 4.12 | 8 | $(8 \times 0) = 0$ |
| P less than 2 percent | 4.12 | 5 | $(4 \times 1) + (1 \times 0) = 4$ |
| P less than 1 percent | 4.16 | 4 | $(4 \times 1) = 4$ |
| P less than 0.5 percent | 4.14 | 5 | $(5 \times 1) = 5$ |
| | | Total Count = | 13 |

The SCHEIE scores are calculated for superior and inferior hemifields as shown in figure 4.23.



$$\text{SCHEIE Score} = \frac{\text{Superior Hemifield}}{\text{Inferior Hemifield}} = \frac{6}{3}$$

Figure 4.23: Superior and Inferior Hemifields scored according to SCHEIE method

4.5 Count of PKSs per ISNT Region

The visual field can be divided into ISNT Quadrants as shown in figure 4.23.

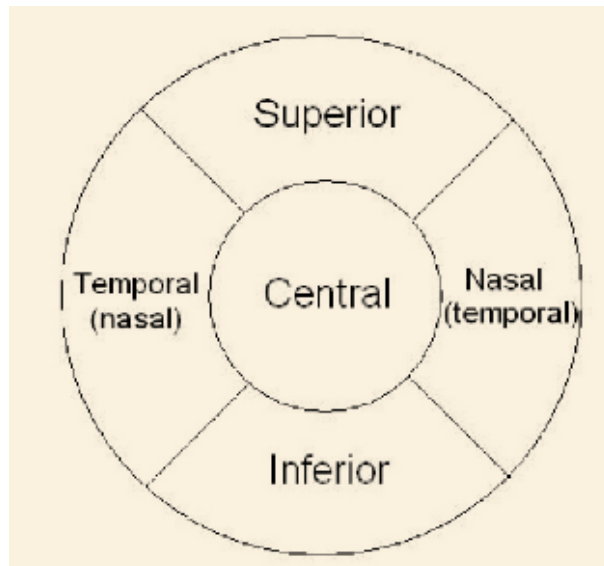


Figure 4.24: Inferior, Superior, Nasal ,Temporal and Central Regions in Optometry[42]

Based on analogy of figure 4.24 we divided the PD region of HVFT into 6 regions: three in superior and three in inferior (paracentral, nasal and temporal) as shown in figure 4.25. Superimposing these 6 regions onto the visual field report results in figure 4.26.

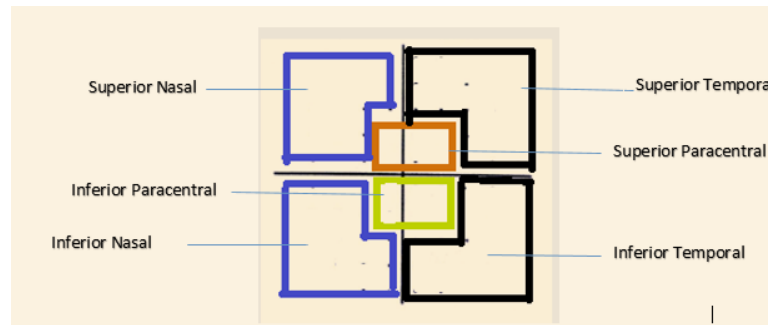


Figure 4.25: Division of PD into 6 Regions

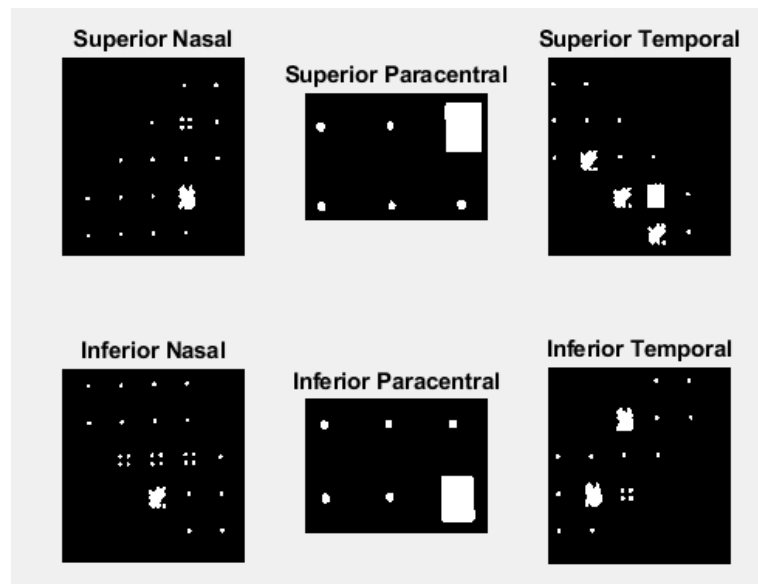


Figure 4.26: Superimposing 6 Regions onto VFT Report

We calculated the scores per ISNT region as well as for 6 regions as shown in figures 4.27 and 4.28.

We are interested in the paracentral region as the loss of central vision is clinically more significant as compared to the loss of peripheral vision. The glaucoma even at an early stage may start with the loss of peripheral vision or central vision or both. The loss of central vision affects the QOL more significantly hence we also attempted to score visual field defects within central 5 degrees of visual field.

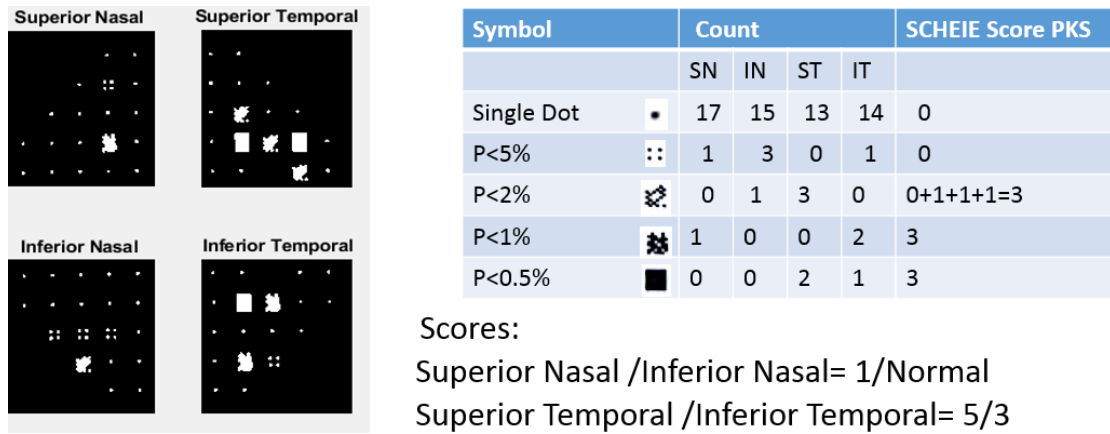


Figure 4.27: Calculation of SCHEIE scores for 4 ISNT regions

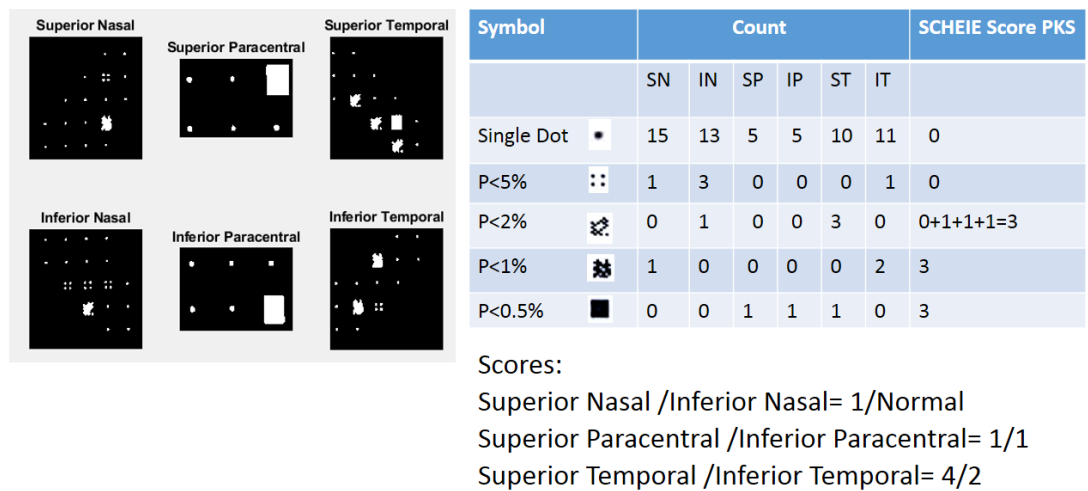


Figure 4.28: Calculation of SCHEIE scores for 6 regions

EXPERIMENTAL RESULTS

5.1 Dataset Description

The proposed algorithm was tested on a local dataset obtained from Armed Forces Institute of Ophthalmology (AFIO), Rawalpindi, Pakistan. The dataset has 50 HVFT RGB images of size 600-700KB scanned and saved as JPEG files. Figure 5.1 shows only the cropped PSD (ROI) for a few images from the dataset showing normal, and glaucamatus eyes(early and advanced). These qualitative annotations were done by the ophthalmologist. The mean age of the patients whose reports were collected is 54.85 having standard deviation of 20.43.

The fixation monitor used was set at **gaze/blindspot** for 30 patients and **Gaze Track** for 1 patient and was set at **Off** for the remaining patients. The fixation target was **central** for all patients. All these tests are performed for monocular vision single field analysis meaning one eye is tested at a time containing 30 right and 20 left eyes. The reports for which fixation losses, false positive and negative errors are more than 33 percent implying that these tests are not reliable for further investigation were discarded. The stimulus size used is **Goldmann size III** and of **white color**. The background luminance is **31.5 asb** and the test strategy was either **SITA** (5 images) or **SITA-FAST** (45 images) using **30 degrees test** . The test duration, date, time, age and name of each patient is recorded in the patient's credentials in each report.

The 30 degrees Humphrey VFT contains a total of 76 test points and containing 19 or 18 points in each quadrant. Similarly, the 24 degrees Humphrey VFT contains a total of 54 test locations where left hemisphere contains a total of 26 points (13 test locations

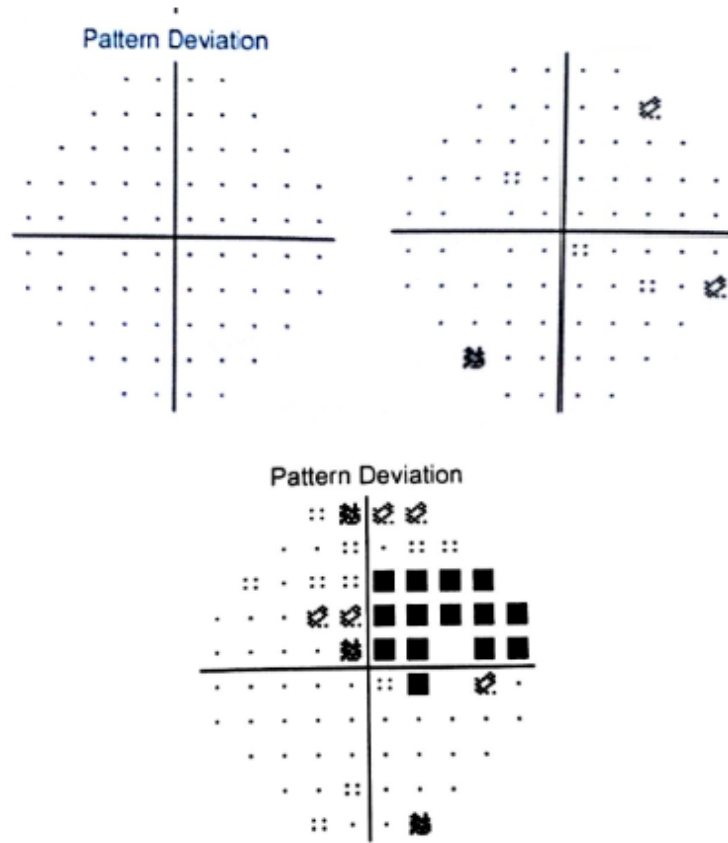


Figure 5.1: (a): Normal Eye (b): Early Glaucoma (c): Severe Glaucoma

each) and the right hemisphere contains 28 points (14 locations each) for both the right and left eye.

Table 5.1: Dataset Used

| Strategy | Total | Normal | Glaucoma | | |
|---------------|-------|--------|----------|----------|----------|
| | | | Early | Moderate | Advanced |
| SITA Fast | 41 | 16 | 15 | 3 | 7 |
| SITA Standard | 5 | 2 | 0 | 2 | 1 |

2 reports were excluded due to poor resolution quality and 2 reports were excluded because of false negative errors greater than 33 percent.

5.2 PKS Extraction

Our algorithm calculates the score of each PKS in the 6 regions as well as their overall count. The first step is the correct labeling of the depressed PKS. In order to segregate PKS we made use of 7 statistical properties as discussed in section 4.3. The mean and std of these attributes is shown in the following table 5.2

Table 5.2: Mean and Standard Deviation of Statistical Features Used for PKS Segmentation

| Symbol | Perimeter | Solidity | Area | Eccentricity | Extent | Major Axis Length | Minor Axis Length |
|------------|----------------------|---------------------|------------------------|--------------------|---------------------|---------------------|---------------------|
| Single Dot | 38.37 ± 1.05 | 0.96 ± 0.005 | 134.81 ± 6.38 | 0.27 ± 0.09 | 0.72 ± 0.03 | 12.86 ± 0.35 | 13.46 ± 0.34 |
| P<5% | 111.21 ± 1.85 | 0.91 ± 0.009 | 795.60 ± 12.96 | 0.52 ± 0.02 | 0.83 ± 0.01 | 30.16 ± 0.39 | 35.52 ± 0.41 |
| P<2% | 142.86 ± 1.88 | 0.90 ± 0.001 | 1211.40 ± 12.19 | 0.43 ± 0.02 | 0.77 ± 0.007 | 38.40 ± 0.37 | 42.67 ± 0.27 |
| P<1% | 140.25 ± 5.64 | 0.85 ± 0.009 | 796.00 ± 25.51 | 0.25 ± 0.03 | 0.78 ± 0.01 | 32.76 ± 0.50 | 33.89 ± 0.25 |
| P<0.5% | 117.19 ± 0.86 | 0.98 ± 0.01 | 970.14 ± 16.20 | 0.29 ± 0.05 | 0.96 ± 0.02 | 35.13 ± 0.51 | 36.78 ± 0.27 |

5.3 PKS Classification

We created ground truth data for all 50 HVFT reports by assigning label to each of the PKS. The algorithm of segregation of PKS was run on the entire data set giving us the detected labels. We then compared the target and detected labels to account for any misclassifications. The 5x5 count confusion matrix for PKS classification is shown as

follows:

$$C = \begin{bmatrix} 2171 & 0 & 0 & 0 & 0 \\ 0 & 168 & 0 & 0 & 0 \\ 0 & 0 & 105 & 0 & 0 \\ 0 & 0 & 0 & 78 & 0 \\ 0 & 0 & 8 & 0 & 141 \end{bmatrix}$$

where, single dots belong to class 1, $P < 5\%$ belong to class 2, $P < 2\%$ belong to class 3, $P < 1\%$ belong to class 4 and $P < 0.5\%$ belong to class 5. Only one image shows 8 false identifications of $P < 0.5\%$ points. The original ground truth image consists of 64 $P < 0.5\%$ points as shown in figure 5.2.

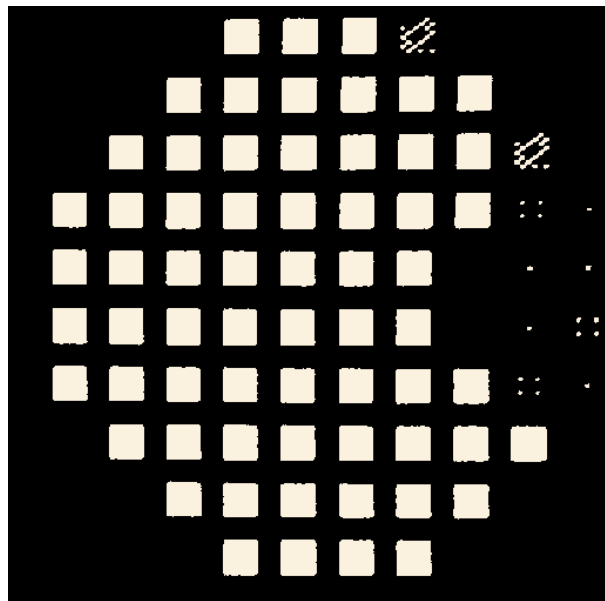


Figure 5.2: Ground Truth for Image 14

After segregation however, the 8 out of 54 $P < 0.5\%$ points are classified as $P < 2\%$ points as shown in figure 5.3.

5.4 Mapping of SCHEIE Scores to Grades

The algorithm calculate the SCHEIE Scores shown in table in each ISNT quadrant and also paracentral superior and inferior quadrants and further mapped these SCHEIE scores into four qualitative grades in each of the 6 regions.

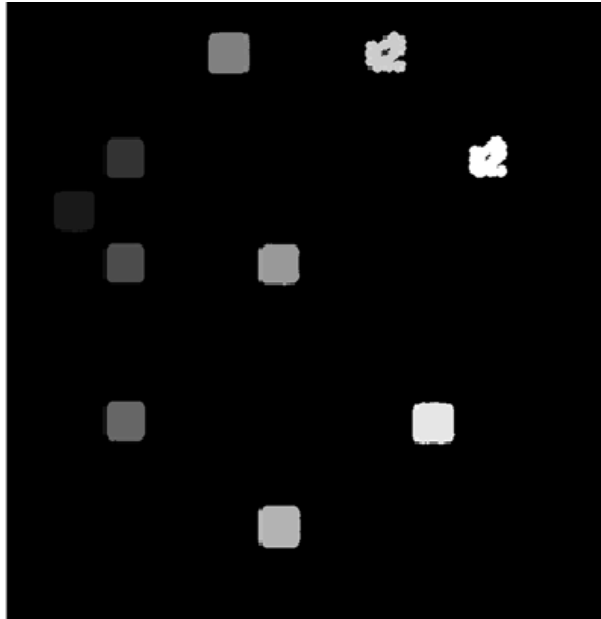


Figure 5.3: Falsely Detected $P < 0.5\%$ for Image 14

- **Normal:** If score in each quadrant is 0.
- **Early Glaucoma:** If score is in the range (1:6)
- **Moderate Glaucoma:** If score is in the range (7:12)
- **Advanced Glaucoma:** If score is ≥ 13

The Paracentral region was graded normal if score was 0, otherwise the paracentral inferior or superior region was graded: "Paracentral Vision being affected" if the score was greater than 0. The following figure 5.4 shows few examples of normal visual fields as graded by the algorithm with scores in all the 6 regions. Figure 5.5 ,5.6 and 5.7 show the examples of early, moderate and advanced glaucoma with SCHEIE scores in all the 6 regions.

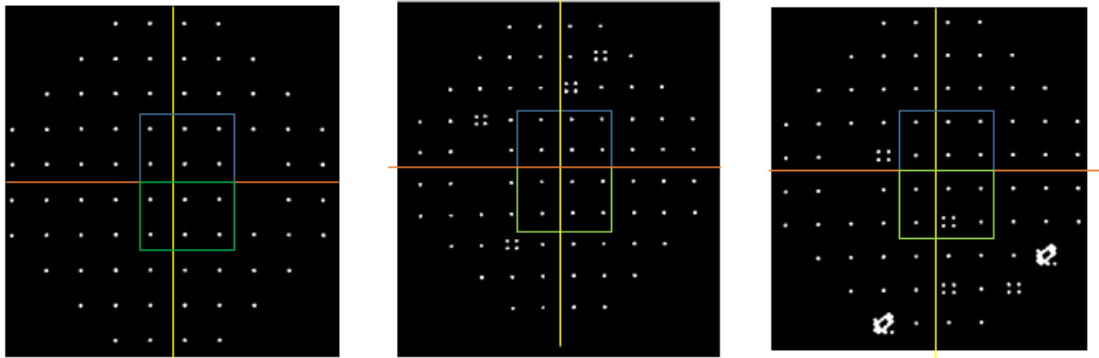


Figure 5.4: Few cases of graded Normal VFs having no glaucoma

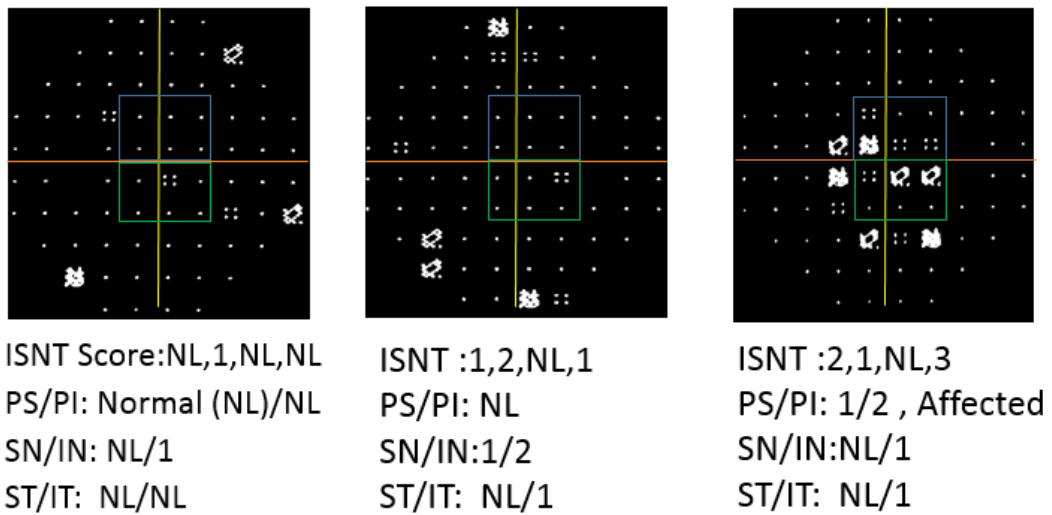


Figure 5.5: Examples of graded VFs showing early glaucoma with individual SCHEIE Scores in all 6 regions

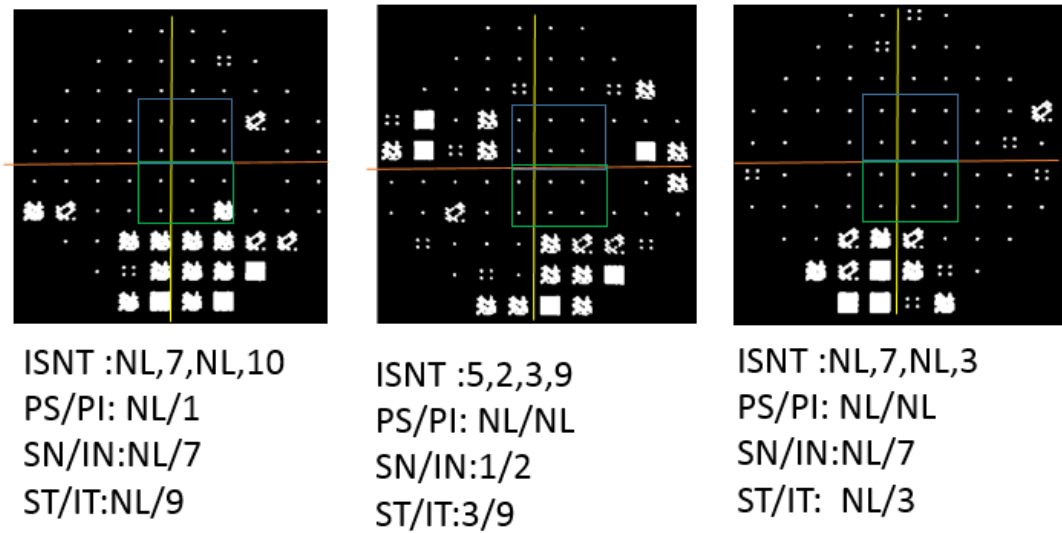


Figure 5.6: Examples of graded VFs showing moderate glaucoma with individual SCHEIE Scores in all 6 regions

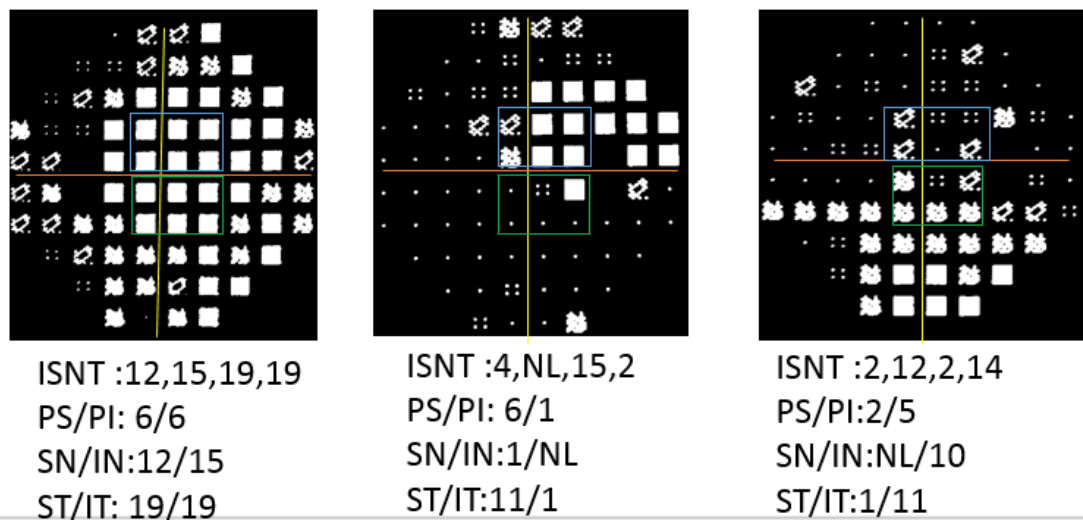


Figure 5.7: Examples of graded VFs showing advanced glaucoma with individual SCHEIE Scores in all 6 regions

CONCLUSION AND FUTURE WORK

6.1 Conclusion

Glaucoma; the second most leading cause of blindness in the world and the one that comes without any symptoms produces structural and functional changes. The structural changes occur in the optic nerve and the functional changes appear in the visual field hence a visual field test is performed to analyze effect of Glaucoma on patient's vision. Traditionally manual analysis of report is being done which requires expertise. In this research, we used image processing and decision support techniques for automated analysis of VFT reports to grade Glaucoma level.

This thesis discussed the algorithm for automatic segmentation of key symbols in HVFT report since this is the first step in order to automate the process of interpretation of VF results to diagnose glaucoma. We used region based properties for connected components to extract the PKS elements in the Humphrey VFT reports. The dataset comprising of 50 VFT reports for varying age groups was obtained and the accuracy of the algorithm was validated by the ophthalmologist. This work is very useful for ophthalmologists as it quantifies the visual field damage in all ISNT quadrants by telling the exact count of each PKS and also its location.

6.2 Contribution

We created a fully automated system for extraction, location and count of PKS in the HVFTs and also extended the work done in calculating SCHEIE scores (which computed scores only in superior and inferior hemifield)[43] by scoring glaucoma in the six regions: superior temporal, superior nasal, inferior temporal, inferior nasal, paracentral inferior and paracentral superior where the scores are proportional to the degree of visual function loss in each of these quadrant regions.

6.3 Future Work

The data set can be increased by acquiring more VFT reports of the patients. We have done this work on images, a data set available is in the form of values of the test location of PSD instead of graphic plot whose data analysis and processing can be done. Also, in this thesis we have implemented our methodology using statistical properties of the PKSs to score glaucoma and describe the extent the deterioration of visual field in the four ISNT quadrants. This work can be extended to the usage of classifiers to determine the characteristic pattern of glaucamatus defect in the HVFT reports. Also this work can be extended for Octopus visual field testing which is also gaining popularity nowadays.

Bibliography

- [1] Zaulaf M., "Normal Visual fields measured with Octopus Program G1.1. Differential light sensitivity at individual test locations", *Graefes Arch Clin Exp Ophthalmol*, 1994;232:509-515.
- [2] Glaucoma research foundation. [Online]. Available: <http://www.glaucoma.org/>
- [3] Sassani JW., "Ophthalmic Fundamentals: Glaucoma.", *Thorofare, NJ: SLACK, c1999*.
- [4] Anderson DR and Patella VM, "Automated Static Perimetry: 2nd Edition. Mosby, Inc., 1999."
- [5] Bayer A and Erb C., "Short Wavelength Automated Perimetry, Frequency Doubling Technology Perimetry, and Pattern Electrorretinography for Prediction of Progressive Glaucomatous Standard Visual Field Defects". *American Academy of Ophthalmology*, 109(5),1009-1017 (2002).
- [6] source: www.nih.gov
- [7] Source:www.eyediologyopticians.co.uk
- [8] Helga Kolb, "Simple Anatomy of the Retina", Book: *Web Vision, The Organization of the Retina and Visual System*
- [9] <https://www.ncbi.nlm.nih.gov/pmc/articles/PMC2814576/>
- [10] Wandell, B. A., "Foundations of Vision ", *Sunderland, Massachusetts: Sinauer Associates, Inc.*
- [11] OpenStax, "Anatomy and Physiology". *OpenStax CNX. 18 May 2016*
- [12] Dr. Hannah de Guzman, "Visual Field Basics"

BIBLIOGRAPHY

- [13] A. D. Chan, "Head-mounted perimetry", *Master's thesis, University of Toronto, 1999*.
- [14] Ilona Wong, "Mobile Perimeter", *Master's thesis, University of Toronto 2016*
- [15] Holz FG, Pauleikhoff D, Klein R, Bird AC., "Pathogenesis of lesions in late age-related macular disease", *Am J Ophthalmol 2004;137:504-510*.
- [16] Collen Kummert, "Statistical modeling to improve the detection of glaucoma progression", *Master's thesis, University of Iowa, Fall 2013*
- [17] Carlos Gustavo V. De Moraes, Viral J. Juthani, Jeffrey M. Liebmann, Christopher C. Teng, Celso Tello, Remo Susanna Jr, Robert Ritch, "Risk Factors for Visual Field Progression in Treated Glaucoma", *Arch Ophthalmol. 2011;129(5):562-568. doi:10.1001/archophthalmol.2011.72, May 12, 2010*.
- [18] Dana M. Blumberg, Carlos Gustavo De Moraes, Alisa J. Prager, Lama Al-Aswad, George A. Cioffi, Jeffrey M. Liebmann, Donald C. Hood, "Association Between Undetected 10-2 Visual Field Damage and Vision-Related Quality of Life in Patients With Glaucoma", *JAMA Ophthalmol. 2017;135(7):742-747. doi:10.1001/jamaophthalmol.2017.1396, July 2017*.
- [19] Pamela A. Sample, Christopher A. Girkin, Linda M. Zangwill, Sonia Jain, Lyne Racette, Lida M. Becerra, Robert N. Weinreb, Felipe A. Medeiros, M. Roy Wilson, Julio De León-Ortega, Celso Tello, Christopher Bowd, Jeffrey M. Liebmann, ADAGES Study Group, "The African Descent and Glaucoma Evaluation Study (ADAGES)", *Arch Ophthalmol. 2009;127(9):1136-1145. doi:10.1001/archophthalmol.2009.187, 2009*.
- [20] Seddon JM, "The differential burden of blindness in the United States", *N Engl J Med 1991;325 (20) 1440- 1442, 1991*
- [21] Sommer, "A Glaucoma risk factors observed in the Baltimore Eye Survey", *Curr Opin Ophthalmol 1996;7 (2) 93- 98, 1996*
- [22] Sommer, "A Epidemiology, ethnicity, race, and risk", *Arch Ophthalmol 2003;121, 2003*

- [23] Christopher A. Girkin, Pamela A. Sample, Jeffrey M. Liebmann, Sonia Jain, Christopher Bowd, Lida M. Becerra, Felipe A. Medeiros, Lyne Racette, Keri A. Dirkes, Robert N. Weinreb, Linda M. Zangwill, ADAGES Group, "African Descent and Glaucoma Evaluation Study (ADAGES)II", *Arch Ophthalmol.* 2010;128(5):541-550. doi:10.1001/archophthalmol.2010.49,2010
- [24] Artes, Iwase, Kitzawa, and Chauhan, "Properties of Perimetric Threshold Estimates from Full Threshold, SITA Standard, and SITA Fast Strategies", *Investigative Ophthalmology and Visual Science*, 43(8), pp. 2654-2659,, 2002.
- [25] Saunders," Studies on real world visual field data in glaucoma", *Doctoral thesis, City, University of London L. J. (2015)*.
- [26] Ryo Asaoka,"Mapping Glaucoma Patients' 30-2 and 10-2 Visual Fields Reveals Clusters of Test Points Damaged in the 10-2 Grid That Are Not Sampled in the Sparse 30-2 Grid " doi.org/10.1371/journal.pone.0098525, June 20, 2014.
- [27] Sung Chul Park, Yungtai Kung,Daniel Su,Joseph L. Simonson, Rafael L. Furlanetto, Jeffrey M. Liebmann, Robert Ritch, "Parafoveal Scotoma Progression in Glaucoma, Humphrey 10-2 versus 24-2 Visual Field Analysis", *Ophthalmology*, presented in part at: *Association for Research in Vision and Ophthalmology Annual Meeting, May 2012, Fort Lauderdale, Florida.*, /doi.org/10.1016/j.ophtha.2013.01.045.
- [28] Dana M. Blumberg, Carlos Gustavo De Moraes, Alisa J. Prager, Lama Al-Aswad, George A. Cioffi, Jeffrey M. Liebmann, Donald C. Hood, "Association Between Undetected 10-2 Visual Field Damage and Vision-Related Quality of Life in Patients With Glaucoma " , *JAMA Ophthalmol.* 2017;135(7):742-747. doi:10.1001/jamaophthalmol.2017.1396,July 2017.
- [29] Carlos Gustavo V. De Moraes, Jeffrey M. Liebmann, Robert Ritch, Donald C. Hood, "Understanding Disparities Among Diagnostic Technologies in Glaucoma" *Arch Ophthalmol.* 2012;130(7):833-840. doi:10.1001/archophthalmol.2012.786, July 2012.
- [30] Yaniv Barkana, Yariv Gerber, Ricardo Mora, Jeffrey M. Liebmann, Robert Ritch,"Effect of Eye Testing Order on Automated Perimetry Results Using the Swedish Interactive Threshold Algorithm Standard 24-2 " *Arch Ophthalmol.* 2006;124(6):781-784. doi:10.1001/archophth.124.6.781, June 2006

BIBLIOGRAPHY

- [31] Jeffrey D. Henderer, "Interpreting Visual Fields, Advice on using staging systems to make informed treatment decisions" *Glaucoma Today* , Aug 2004.
- [32] Susanna Jr, Remo, and Roberto M. Vessani, "Staging glaucoma patient: why and how?" *The open ophthalmology journal 3 (2009): 59.*
- [33] Rasker, Marga TE, et al.i, "Rate of visual field loss in progressive glaucoma", *Archives of ophthalmology 118.4 (2000): 481-488.*
- [34] Chakravarti, Tutul, "Assessing Precision of Hodapp-Parrish-Anderson Criteria for Staging Early Glaucomatous Damage in an Ocular Hypertension Cohort: A Retrospective Study", *Asia Pac J Ophthalmol (Phila) (2016).*
- [35] Ng, Minna, et al , "Comparison of visual field severity classification systems for glaucoma," *Journal of glaucoma 21.8 (2012): 551.*
- [36] M. Ng, P.A. Sample, J.P. Pascual, L.M. Zangwill, C.A. Girkin, J.M. Liebmann, R.N. Weinreb, and L. Racette , "Comparison of visual field severity classification systems for glaucoma," *HHS Author Manuscripts PMC3246042 Oct 1, 2013*
- [37] Gonzalez, R.C., Woods, R.E., " Digital Image Processing. *Addison-Wesley Longman Publishing Co., Inc.; 1992.*
- [38] <https://sites.ualberta.ca/~ccwj/teaching/image/morph/>
- [39] <https://blogs.mathworks.com/steve/2010/08/16/isotropic-dilation-using-the-distancetransform>
- [40] Michael B. Dillencourt; Hannan Samet; Markku Tamminen (1992). "A general approach to connected-component labeling for arbitrary image representations"., *Journal of the ACM. J. ACM. 39 (2): 253. doi:10.1145/128749.128750.*
- [41] Sankar, Prithvi S. et al. "The SCHEIE Visual Field Grading System." , *Journal of clinical and experimental ophthalmology 8.3 (2017): 651. PMC. Web. 18 Sep. 2017.*
- [42] <https://doi.org/10.3341/jkos.2007.48.12.1623>
- [43] Boland, et.al. , " Quantitative Analysis of the Displacement of the Anterior Visual Pathway by Pituitary Lesions and the Associated Visual Field Loss." , *Investigative Ophthalmology and Visual Science. 57. 3576. 10.1167/iops.16-19410.,(2016*